6.4 Wavelength Tuning of Intersubband Absorption in GaN/AlN Multiple Quantum Wells Grown on AlN

As mentioned in the last section, the intersubband absorption wavelength in GaN/AlN MQW grown on AlN-based waveguide is quite difficult to control because of the large built-in electric field induced by stress in GaN quantum wells. In order to tune the wavelength of absorption, three methods are described as follows:

1) Changing quantum well thickness

As the subband energy levels make a shift in energy with increasing or decreasing of quantum well thickness, the change of quantum well thickness should be the easiest way to change the energy levels. However, since a little change of thickness could not be used to adjust the absorption wavelength, a large increase in thickness is required for the wavelength adjustment. It is also difficult to adjust the absorption wavelength to long wavelength side because the thickness must be increased to be over the critical thickness, which could cause crystalline defects in the quantum well structure.

2) Changing barrier height

The AlN barrier normally gives the highest barrier for nitride-based quantum wells. The use of AlN thus results in the shortest intersubband transition wavelength in case of GaN quantum wells. The tuning of intersubband absorption wavelength to long wavelength can therefore be performed by changing the barrier from AlN to AlGaN, resulting in lower barrier and a red shift of the intersubband absorption wavelength. Because the lattice mismatch in AlGaN is smaller than in AlN barrier, changing the barrier to AlGaN also affect in a decrease of lattice-mismatch induced stress in the quantum well, making it easier to grow the MQW structure. This method can therefore be used to adjust the intersubband absorption wavelength of the AlN-based waveguide. However, changing the barrier height might require some upgrade of growth machine, as two GaN source will be required in the growth of both AlGaN barrier and GaN quantum well. It is thus not possible to be performed in this study.

3) Changing barrier thickness

The indirect way to adjust the intersubband transition wavelength is to adjust the barrier thickness, which could result in the change of the built-in electric field. Since it is known that the built-in electric field in the AlN waveguide is too large, the shift to long-wavelength side could therefore be achieved by reducing the strength of the built-in electric field, which can be performed by decreasing the barrier thickness.

In this study, the wavelength adjustment was firstly performed by changing the quantum well thickness. Figure 6.11 shows the transmission spectra of three samples with well thickness varied by 2.5 nm, 3.3 nm and 4.0 nm, while the barrier thickness was kept constant at 10.5 nm. As can be seen in the figure, the wavelength of intersubband absorption shifted from 1.35 μm to 1.52 μm and 1.70 μm with stronger absorption for a change in the quantum well thickness from 2.5 nm to 3.3 nm and 4.0 nm, respectively. As expected, stronger absorption was observed for thicker quantum well, because the number of carrier in quantum wells generally increase with thicker quantum well, thus inducing stronger absorption. This result is in good agreement with the prediction that the wavelength should be shifted when the quantum well thickness is

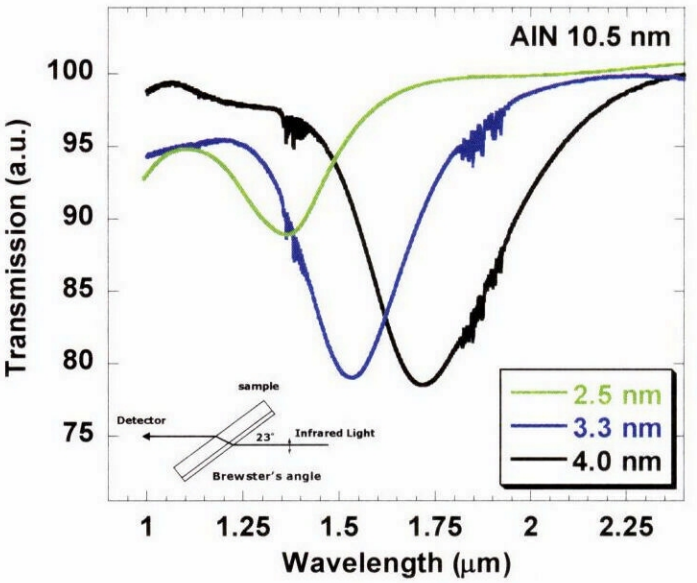

Figure 6.11 Wavelength tuning of intersubband absorption in GaN/AlN MQW grown on AlN by changing quantum well thickness.

thicker than the critical thickness, causing lattice relaxation in the GaN quantum wells. As a result, the built-in electric field in the GaN is weakened. This result also confirmed the assumption that the intersubband absorption of quantum wells thinner than 2.5 nm is difficult to tune the wavelength because of the effect of built-in electric field.

The other method for adjusting the wavelength of intersubband absorption, changing barrier thickness, is also studied here. The well thickness was fixed at 3.3 nm which is thicker than the critical thickness, while the barrier thickness was varied by 3 nm, 10.5 nm, and 31.5 nm. The transmission spectra of three samples are shown in Fig. 6.12. It can be obviously seen that the wavelength can be adjusted by changing the barrier thickness. For thick barrier, the absorption wavelength shifted to shorter wavelength as predicted, owing to the stronger built-in electric field. On the other hand, the absorption wavelength shifted to longer wavelength for thin barrier as a result of weakening electric field. However, the amount of absorption became smaller for 30-nm-thick barrier samples, which is thought to be a cause of crystalline defects as the growth of thick AlN barriers with high quality is still not possible by MBE growth technique.

Considering these results, it can be concluded that the intersubband absorption wavelength in thick GaN quantum wells grown on AlN buffer layer can be tuned with

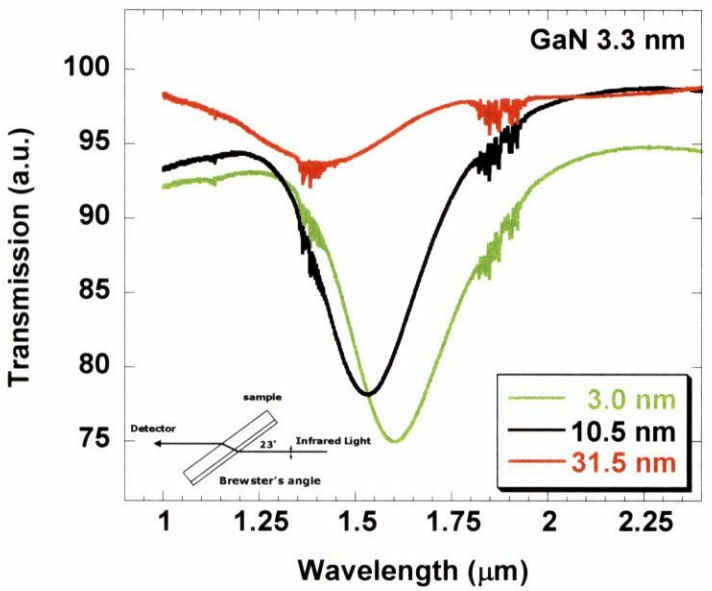

Figure 6.12 Wavelength tuning of intersubband absorption in GaN/AlN MQW grown on AlN by changing barrier thickness

changing the strength of built-in electric field. However, the built-in electric field cannot be adjusted directly, but requires the change of quantum well thickness or barrier thickness instead. It is therefore necessary to understand the crystal-growth ability and nature of built-in electric field very well in order to tune the absorption wavelength to the desired wavelength for MQW on AlN buffer layer.

6.5 Ultrafast All-Optical Switch Operating at 1.55 μm

In order to fabricate the intersubband transition device that operates at 1.55 μm, as described in the last section, it is needed to increase the quantum well thickness to be thicker than the critical thickness of GaN on AlN layer. With such thickness, the lattice relaxation can induce the defects such as threading dislocation inside the quantum wells, resulting in large switching energy of the input optical pulse to achieve the intersubband absorption saturation. The optimal barrier thickness that can grow the MQW structure with low defect density should therefore be investigated. In addition, the optical confinement of the core should also be carefully considered. As described in Chapter 5, the total thickness of the core is needed to be as thick as possible in order to increase the optical confinement of the core, while low carrier concentration is required to reduce the amount of absorption, which could result in a reduction of the switching energy. However, since the MQW composing of lattice-mismatched materials, too thick core can generate defects with high density. The quantum well thickness, barrier thickness, total core thickness, and the carrier concentration are therefore very important parameters needed to be concerned for the fabrication of 1.55-μm intersubband transition devices based on AlN waveguide structure. In order to investigate such parameters, the AlN waveguides with GaN/AlN MQW fabricated with different parameters as shown in Table 6.1 were fabricated and characterized for the intersubband absorption saturation. Firstly, the effect of quantum well thickness is investigated using Waveguide A and B. Waveguide A is the first AlN-waveguide-based intersubband transition device operating at 1.3 μm as described in Section 6.1 to 6.3, while Waveguide B was fabricated with the same structure but the GaN quantum well

Table 6.1 Structures of AlN waveguides with different GaN/AlN quantum well structure

Waveguide	GaN Quantum Well Thickness (nm)	AlN Barrier Thickness (nm)	Number of Quantum	Doping (cm^{-3})	Observed Absorption Saturation
A	2.0	10.5	2	1×10^{20}	7dB @200pJ
B	3.3	10.5	2	1×10^{20}	-
C	3.6	10.5	20	5×10^{18}	2dB @100pJ
D	3.3	31.5	10	1×10^{19}	2dB @100pJ
E	3.3	3.3	10	1×10^{19}	1dB @100pJ
F	3.3	3.3	5	1×10^{19}	10dB @90pJ

thickness was changed to 3.3 nm to obtain the intersubband absorption at about 1.55 μm. In contrast to the observation of 7-dB absorption saturation in Waveguide A, Waveguide B provides very high TM-mode propagation loss, making it not possible to detect the absorption saturation. Such high TM-mode propagation loss is thought to be due to an increase in the defect density as the thickness of GaN quantum wells was increased to be thicker than the critical thickness. Additionally, since the thickness was increased, the amount of carriers inside the quantum well increased, resulting in stronger intersubband absorption at 1.55 μm.

Next, the optimal barrier thickness is investigated using Waveguide C, D and E. To reduce the amount of intersubband absorption and to increase the core optical confinement, the carrier concentration in the GaN quantum well was reduced to be 5×10^{18} cm^{-3} in Waveguide C, and 1×10^{19} cm^{-3} in Waveguide D and E, while the amount of quantum wells was increased to be 20 and 10, respectively. The intersubband absorption in these samples was found at about 1.6 μm, comfirmed by both the Multiple-reflection method and the Waveguide-coupling method. However, only 1-2 dB of intersubband absorption saturation was observed in the samples cleaved with a waveguide length of 400 μm. The effect of barrier thickness is then investigated by the Waveguide-coupling method as shown in Fig. 6.13 for Waveguide D and E, which has almost the same structure except the barrier thickness. As seen in Fig. 6.13, both samples have broad absorption spectrum, suggesting that the absorption might be still too strong. Note that the maximum distinction ratio that can be observed by the Waveguide-coupling intersubband-absorption measurements is limited by the distinction ratio of the polarizer used in the experiment. In this study, the maximum

distinction ratio is estimated to be about 25 dB, meaning that absorption stronger than 25 dB can cause a broad absorption peak with this method.

However, the important difference observed between Waveguide D and E is the TM/TE propagation loss ratio in the wavelength range of 1.1-1.2 μm, where Waveguide E shows TM/TE ratio of almost zero, while Waveguide D shows 5-10 dB difference. In general, this wavelength range is expected not to contain intersubband absorption; it is thus used to characterize the waveguide quality as described in Chapter 4 and 5. The 5-10 dB of TM/TE ratio is therefore thought to be due to the extra TM-mode propagation loss, which is caused by crystalline defects generated during the growth of lattice-mismatched MQW layer. Since Waveguide D contains thick barrier (31.5 nm) compared with quantum well (3.3 nm), the stress induced in the GaN quantum well is expected to be strong, causing high density of crystalline defects in Waveguide D. On the other hand, Waveguide E was fabricated with the same barrier and quantum well thickness (3.3 nm), making the average Al-composition of the MQW layer in Waveguide E becoming about 50%, which means that the stress induced in the GaN quantum well is much reduced in Waveguide E compared with Waveguide D. Therefore, the density of crystalline defects in Waveguide E is expected to be much reduced in Waveguide E, providing no extra TM mode propagation loss. Considering these results,

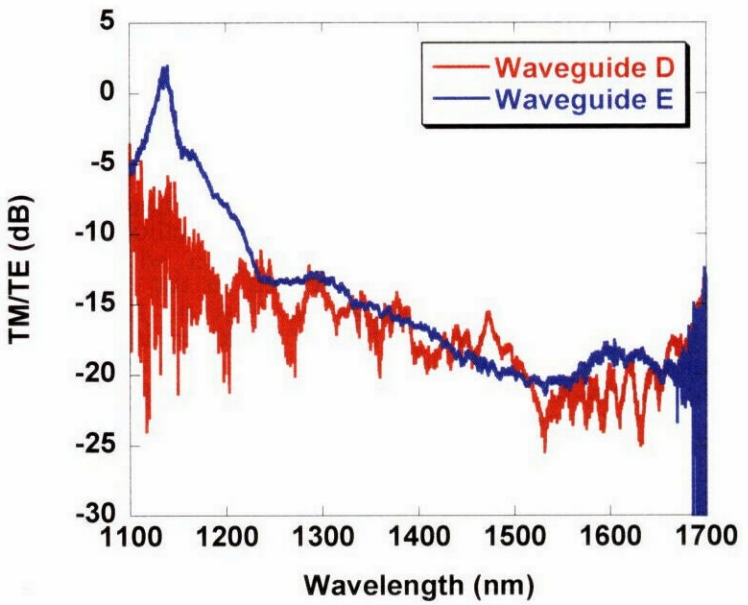

Figure 6.13 Intersubband absorption spectrum measured by Waveguide-coupling method. of AlN waveguides with different AlN barrier. D: 31.5 nm, E: 3.3 nm.

it can be concluded that the MQW layer should be fabricated with careful consideration of stress induced by lattice mismatch to minimize the defect density, which can be achieved by reducing the barrier thickness to be equal to that of GaN, or by reducing the total MQW thickness.

Finally, to reduce the amount of intersubband absorption in the waveguide, and to reduce the defect density generated in the MQW layer, Waveguide F is fabricated with

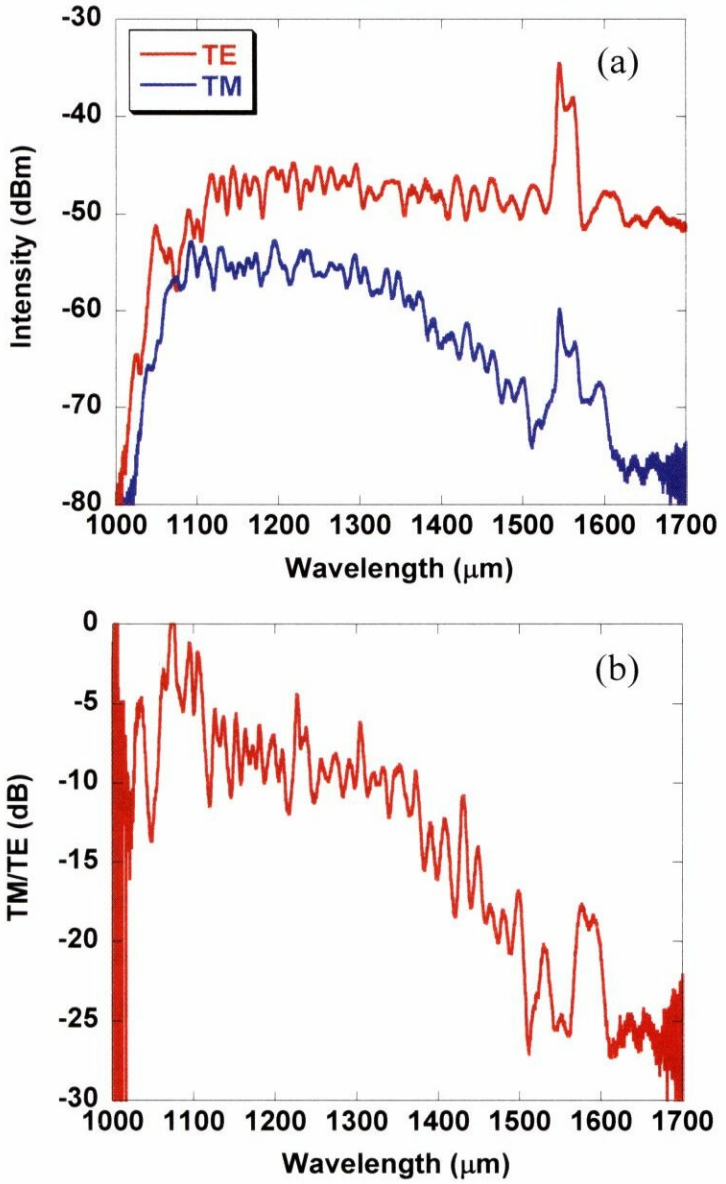

Figure 6.14 (a) TM and TE mode transmission spectra of as-fabricated AlN high mesa waveguide measured by Waveguide-coupling method.
(b) Intersubband absorption spectrum calculated from (a)

the same condition as Waveguide E but the amount of quantum wells is reduced to 5. The intersubband absorption and TM-mode propagation loss in Waveguide F was investigated by Waveguide-coupling method for a waveguide length of 1 mm, as shown in Fig. 6.14.

As seen in Fig. 6.14, clear intersubband absorption can be clearly observed, but the peak wavelength is not clearly confirmed due to the range of measurements. However, it is expected to be longer than 1.65 μm. This absorption peak is much narrower than that of Waveguide D and E. Moreover, at a wavelength of 1.05 μm, the TM/TE propagation loss ratio becomes less than 5 dB, indicating that the waveguide quality is much improved in Waveguide F. The extra TM-mode propagation loss of 5 dB is thought to be due to the defects in the upper AlN cladding layer, as this layer was grown by MBE technique with a thickness of 1 μm. In contrast to GaN, the growth of thick AlN by MBE technique still provides a high density of defects, such as Al droplets.

To confirm the improvement of waveguide characteristic shown in Fig. 6.14, the intersubband absorption saturation is investigated for Waveguide F (600 μm) with the experimental setup described in Section 6.3.1. In Fig. 6.15, the 1.55-μm intersubband absorption saturation characteristic of Waveguide F is illustrated. For TE-polarization, the insertion loss is almost constant at approximately 10.5 dB with increasing input pulse energy from 0.01 pJ to 100 pJ. On the other hand, for TM-polarization, the insertion loss changes from -30 dB to -20, or 10-dB of absorption saturation, with increasing pulse energy. Note that this device is not mounted as a module, so the vibration can cause a shift in energy as seen for TE-polarization in Fig. 6.15. Nevertheless, this result obviously shows that the intersubband absorption saturation by 10 dB was achieved with the input pulse energy of 90 pJ, which is the smallest energy ever reported for the nitride-based intersubband transition devices. It is believed that the characteristic can be further improved with the AR coating and module fabrication [62]. Without such module fabrication, the 3-dB absorption saturation can be obtained with the input pulse energy as small as 8 pJ, much lower energy than that is necessary for GaN-based waveguide (40 pJ) reported in the literature [62]. Therefore, these results indicate that the AlN waveguide structure is a promising structure for improving the switching characteristic of the ultrafast all-optical switch utilizing intersubband transition.

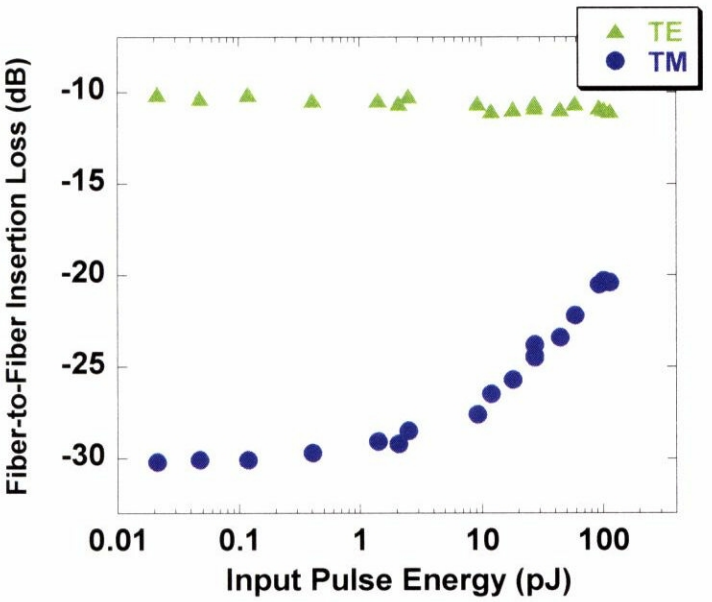

Figure 6.15 Fiber-to-fiber insertion loss of TM and TE polarization of Waveguide F as a function of input pulse energy. 10 dB of intersubband absorption saturation is observed with input pulse energy of 90 pJ.

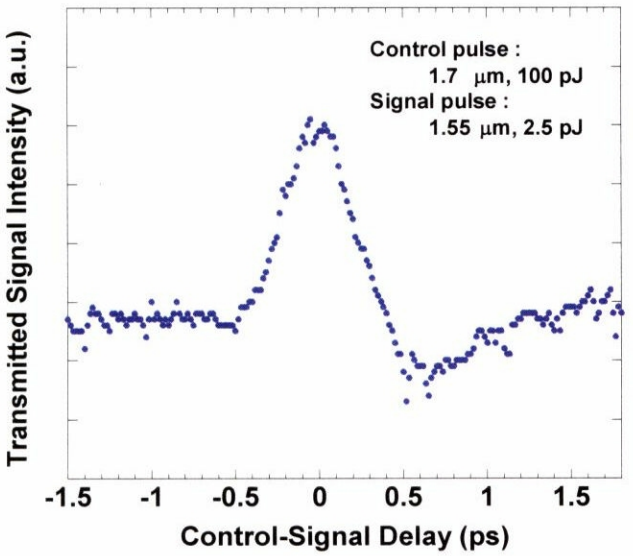

Figure 6.16 Results of pump-probe measurements for Waveguide F

The intersubband absorption saturation measurements was also performed for 1.7 μm, but less than 2 dB of distinction ratio was observed, suggesting that the amount of absorption is very large at the absorption peak, which could be around 1.7 μm or longer

wavelength. The two-color pump-probe measurements have been performed to demonstrate the ultrafast all-optical switching utilizing intersubband transition. Figure 6.16 shows the results of the pump-probe measurements for Waveguide F. The energies of the control (1.7 μm) and the signal pulses (1.55 μm) were 100 pJ and 2.5 pJ, respectively. The cross correlation between these two pulses provide the full width at half maximum (FWHM) of 270 fs. Since the waveguide is not mounted as a module, the measurement on ultrafast all-optical switching is very sensitive to vibration, making it very difficult to obtain a clear switching characteristic. Nevertheless, the result in Fig. 6.16 shows an increase in transmitted signal intensity of around 2 dB when the timing of the control and signal pulse coincides. The FWHM of the switching gate measured in this experiment is estimated to be 440 fs. However, since the pump and signal pulses are not optimized to obtain the shortest pulses, the switching gate is expected to be narrower with optimized pump and signal pulses. These results thus indicate that the ultrafast all-optical switching can be performed successfully with the fabricated device. Therefore, this is the first demonstration of the ultrafast all-optical switching by AlN-waveguide-based intersubband transition devices.

Even though the switching characteristic is not the best compared to the previously reported intersubband transition devices, the AlN-waveguide-based ultrafast all-optical switch is expected to have much better characteristic with the optimization of the structure, absorption wavelength, and module fabrication. These results not only demonstrate the ultrafast all-optical switching utilizing intersubband transition, but also indicating that AlN waveguide structure is a promising structure for the improvement of the switching characteristic of intersubband transition devices.

6.6 Discussions on Switching Pulse Energy

Although the AlN-waveguide-based ultrafast all-optical switch described in Section 6.5 has demonstrated the intersubband absorption saturation with good characteristic better than the GaN-waveguide-based all-optical switches [61,62], the optical pulse energy required for the absorption saturation is still large compared with conventional all-optical switches [176-182]. However, since the device described in Section 6.3 was still not optimized for application as all-optical switch, it is believed that with the optimization of device structure and the tuning of the wavelength, AlN-waveguide-based intersubband transition switches can provide better switching characteristics. This is because AlN waveguide structures have many advantages in developing the intersubband transition devices as follows:

1) Ability to fabricate the high-optical-confinement waveguide structures
2) Low propagation loss waveguide
3) Good carrier confinement to quantum wells
4) Strong built-in electric field in quantum wells

These advantages are special feathers for the intersubband transition devices based on AlN-waveguide structure. They should be optimized to obtain the best performance intersubband transition devices. In this section, two parameters, *switching speed and insertion loss*, are also discussed. These parameters are very important that they should be concerned not only for the AlN-waveguide-based intersubband transition devices, but also for intersubband transition devices fabricated by other structures and other material systems.

Effect of Switching Speed (carrier life time) on Switching pulse energy

In order to study the relation between the switching speed and switching pulse energy, the saturation intensity of the intersubband transition switch is examined [56].

$$I_S \alpha \frac{n_c n_w \pi^2 h \nu_0 \Delta \nu}{2\tau \int \alpha(\nu) d\nu} \qquad (6.1)$$

where, n_c is the sheet carrier density, n_w is the number of wells, $h\nu_0$ is the peak energy, $h\Delta\nu$ is the homogeneous linewidth, τ is the energy relaxation time and the area under the absorption peak is given by $\int\alpha(\nu)d\nu$.

In the above equation, all the terms excepting τ can be estimated from the absorption spectra. The saturation intensity can therefore be written as

$$I_S \alpha \frac{1}{\tau} \qquad (6.2)$$

meaning that the saturation intensity is inversely proportional to the energy relaxation time. From this relation, it can be thought that to operate a switch with fast operating speed (or short response time), high pulse energy is required to pump the waveguide to saturation state. The experimental switching energy of each optical switch is therefore plotted versus the response time in Fig. 6.17. It can be seen that all intersubband transition switches have almost the same relation between switching energy and response time, less than 10 pJ•ps. This relation is no big difference even for the electro-absorption modulators, or SOA-based switches. It is therefore a trade-off between the switching speed and the switching energy. If the switching speed is

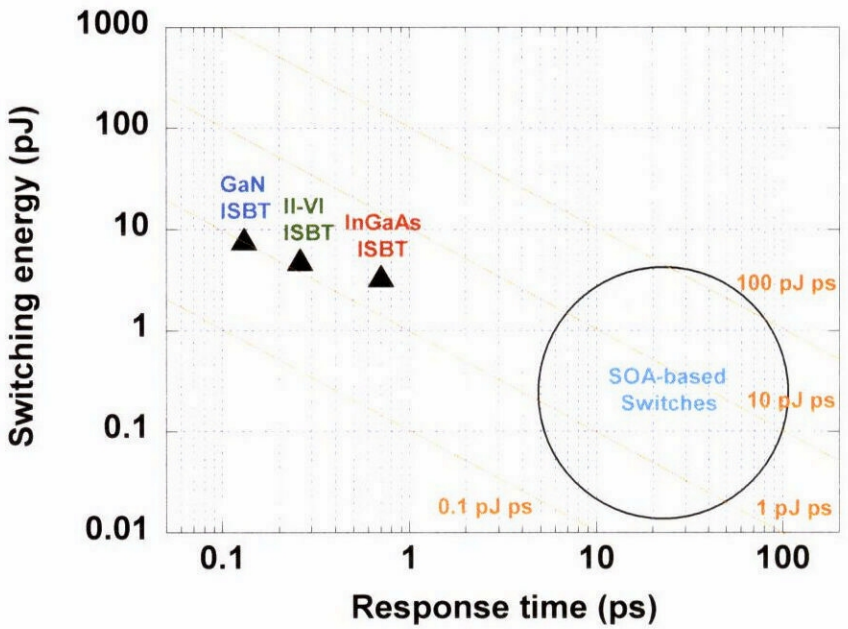

Figure 6.17 Relation between switching energy and response time of all-optical switches. Triangle: Experimental results of intersubband transition switches at 3-dB absorption saturation, Orange line: reference line for "energy×time" value.

required, large switching power will be necessary. In case of GaN quantum wells, the intersubband relaxation time is the shortest among other materials, suggesting that requirement of large switching energy is inevitably. However, reduction of switching energy can still be achieved with optimization of quantum wells. As can be seen in Eq. 6.1, the absorption intensity is proportional to the carrier density and the quantum well number. A decrease in switching energy can thus be achieved by reducing the carrier density.

Effect of Insertion Loss on Switching Pulse Energy

Even though it is known that high switching energy is required for ultrafast switching using intersubband absorption saturation in GaN/AlN MQW, another parameter that should be further studied to reduce the switching energy is the total insertion loss of the waveguide. As described in previous section, the total insertion loss includes the fiber-to-waveguide coupling loss and the propagation loss.

The fiber-to-waveguide coupling loss is usually varied with reflectance of waveguide facet which is different by material. Since AlN has small refractive index, the facet reflectance is smaller than other materials, thus producing lesser coupling loss for the waveguide that is well designed and fabricated. The coupling loss is estimated to be around 10 dB for AlN waveguide coupled by taper fiber. However, the coupling loss could be further bit improved by fabricating a waveguide module coupled by collimating lens, which is expected to be around 3-5 dB.

On the other hand, the propagation loss composes of three parameters which are explained as follows:

1) *Original waveguide propagation loss* is the loss for both TM and TE-polarization generated inside the waveguide due to abnormal shape of waveguide such as sidewall roughness. This loss could be reduced by improving fabrication process to obtain the waveguide with smooth sidewall.

2) *Intersubband Absorption loss* is the TM-polarization loss that is generated by intersubband absorption of quantum wells. This loss is the most important because it is the parameter that directly relates to the On-Off distinction ratio of the switches. For high distinction ratio, this loss should be high, which can be adjusted by increasing the

doping concentration or increasing a number of quantum wells. In that case, higher switching energy is required, and too high loss could results in too large absorption saturation energy. In order to achieve low switching energy, this part should be optimized to be as low as possible while the distinction ratio can be achieved around 10 dB. Such optimization should be performed for both the carrier concentration in the quantum wells and the amount (total period) of quantum wells.

3) *Extra propagation loss generated by crystalline defects* is the TM-polarization loss that is not desirable to exist in any waveguide, because this loss only increases the switching energy without improving the distinction ratio of the switch. This loss must therefore be reduced to be as small as possible, which can be performed by improving the growth technique to obtain high crystalline quality waveguide structure. This loss can be as large as 20 dB for bad crystalline-quality waveguide structure, whereas it can be negligible for the perfectly grown crystal.

In conclusion, the reduction of switching energy is still an important issue for the realization of ultrafast all-optical switching in GaN/AlN MQW. For the low-switching-energy all-optical switches, the optimization of the TM-polarization intersubband absorption loss should therefore be concerned together with the improvement of crystalline quality and waveguide fabrication process. The switching energy can be further improved by making a device module which could improve the coupling loss of the devices.

6.7 Concluding Remarks

In this chapter, the fabrication of ultrafast all-optical switch utilizing intersubband transition was demonstrated by using AlN waveguide structure with GaN/AlN multiple quantum wells. In Section 6.1, the MBE growth of GaN/AlN multiple quantum wells on MOVPE-grown AlN layer was studied. It was found that there exists very strong built-in electric field induced in the GaN quantum wells owing to the large lattice mismatch between GaN and AlN. This built-in electric field is useful for shortening the wavelength of intersubband absorption. By making use of this strong built-in electric

field, the waveguide structure with GaN/AlN quantum wells could be fabricated for a certain intersubband absorption wavelength, without wavelength shifting caused by a change in built-in electric field, especially for a wavelength shorter than 1.4 μm. In Section 6.2, the intersubband absorption at a wavelength as short as 1.3 μm was therefore demonstrated in the AlN waveguide structure with GaN/AlN quantum wells for the first time. This wavelength is the shortest ever reported in the waveguide structure. In Section 6.3, the intersubband absorption saturation in the device was demonstrated by pump-probe measurements using ultrashort optical pulse. 7 dB of absorption saturation was observed for input optical-pulse energy of 200 pJ.

In addition to the demonstration of intersubband transition device based on AlN waveguide at a wavelength of 1.3 μm, in Section 6.4, the wavelength tuning of the device was also demonstrated by changing the quantum well and barrier thicknesses with a careful consideration of the built-in electric field in the quantum wells, leading to the realization of longer wavelength including 1.55 μm. Although it is the first device that can operate in the optical wavelength range of 1.3-1.55 μm, the ultrafast optical-switching characteristic of this AlN-waveguide-based device measured by pump-probe measurements is good, comparable to the GaN-waveguide-based devices previously reported. In Section 6.5, the first AlN-waveguide-based ultrafast all-optical switch operating at 1.55 μm was demonstrated with the careful concern of AlN barrier thickness and optical confinement of the waveguide structure. The switch has very good saturable absorption characteristic at a wavelength of 1.55 μm: input pulse energy of 90 pJ for 10-dB saturation, which is better than that of the conventional GaN-waveguide-based ultrafast all-optical switch.

Such achievements were originated from the characteristic of AlN waveguide structure and the successes in fabricating the structure with high quality. With additional improvement of the waveguide structure and a careful wavelength-tuning, the AlN-waveguide-based device is expected to have much better characteristic for applications on ultrafast all-optical switching. In Section 6.6, the parameters that affect the switching energy of the device were discussed. The switching energy can be reduced by further improvements of crystalline quality and waveguide fabrication which affect the insertion loss. Such improvements are therefore required for the fabrication of the intersubband transition devices with low switching energy.

CHAPTER 7

CONCLUSIONS

In this dissertation, the GaN/AlN multiple quantum wells and nitride-semiconductor-based waveguide structures were studied and fabricated for the applications of ultrafast all-optical switch utilizing the intersubband transition. The ultrafast intersubband transition device was realized by using AlN waveguide structure with GaN/AlN quantum wells. This AlN-waveguide-based intersubband transition device can operate in the optical communication wavelength range, and is the first intersubband transition device that can be designed to cover both 1.3 μm and 1.55 μm. The device was successfully fabricated with a combination of many techniques achieved in both the epitaxial growth of nitride-based semiconductors including their multiple quantum well

structures and the fabrication of the nitride-based waveguide structures. Additionally, the careful design of waveguide structures with materials that has many outstanding properties suitable for intersubband transition devices, GaN and AlN, has led to the successful demonstration of the intersubband-transition ultrafast all-optical switches with high performance.

In Chapter 1, the study began with basic background of the intersubband transition and importance of nitride semiconductors for intersubband transition devices. The interesting characteristics of the intersubband transition and three applications, including quantum well infrared photodetector, quantum cascade laser and ultrafast all-optical switch, were introduced. The chapter was focused on the materials with large conduction-band offset, especially on GaN/AlN multiple quantum wells, since they can provide the intersubband transition at 1.55 μm for fabrication of ultrafast all-optical switch. The difficulty in obtaining the intersubband transition at 1.55 μm for metalorganic vapor phase epitaxy technique and the need of a high-quality waveguide structure for device fabrication were also introduced.

In Chapter 2, the epitaxial growth of nitride-based semiconductors and GaN/AlN multiple quantum wells with metalorganic vapor phase epitaxy technique was described. The high quality GaN was successfully grown with low-temperature nucleation layer technique. The Si-doping of GaN was also achieved with a carrier concentration as high as 9×10^{18} cm^{-3}. It was found that the GaN/AlN multiple quantum well structures face many difficulties to grow with high quality owing to a large lattice mismatch of 2.6% and a difference in temperature coefficient of expansion between GaN and AlN. The growth of GaN/AlN multiple quantum wells therefore requires a special technique such as the insertion of "intermediate layer" to improve the structural quality. The growth of high quality GaN/AlN multiple quantum wells with molecular beam epitaxy technique was also performed and described. By comparing the crystalline and structural quality obtained with both growth techniques, it was found that metalorganic vapor phase epitaxy is more preferable to grow a thick epilayer since it can grow thick epilayer with high crystalline quality as many growth techniques are available to reduce crystalline defects, for example, low-temperature nucleation layer and insertion of intermediate layer. On the other hand, molecular beam epitaxy is more suitable for the growth of

multiple quantum wells since it can grow very sharp quantum-well interfaces and it has ability to suppress the generation of cracks for the growth of large lattice-mismatched material.

In Chapter 3, four methods of intersubband absorption measurements, including Single-pass transmission method, Attenuated total reflection method, Multiple reflection method and Waveguide coupling method, were introduced. Each measurement method was described and found that the measurements with multiple reflection method have a good sensitivity in the detection of intersubband absorption. Using the multiple reflection method, the wavelength tunability of intersubband transition was demonstrated by changing the quantum well width. It was also found that there exists very strong built-in electric field in the quantum wells mainly due to the stress-induced piezoelectric field. Another way to tune the intersubband transition wavelength, adjusting the strength of built-in electric field, was therefore demonstrated by changing the barrier thickness. With optimization of the growth condition, the near-infrared intersubband transition in GaN/AlN multiple quantum wells grown by metalorganic vapor phase epitaxy was achieved with the shortest wavelength of around 2 μm. To obtain the intersubband absorption at shorter wavelengths to cover the optical communication wavelength range, the molecular beam epitaxy was utilized. It was confirmed that the molecular beam epitaxy is suitable for the growth of multiple quantum wells as the intersubband absorption 1.55 μm was easily obtained. It was also clarified that the growth with metalorganic vapor phase epitaxy still cannot provide perfectly-sharp-interface quantum wells, while such quantum wells can be grown without difficulty with the molecular beam epitaxy.

In Chapter 4, the fabrication of GaN-based waveguide structures was studied. Several waveguide structures were proposed and investigated for their possibilities to use as a waveguide structure for the intersubband transition device. It was found that to obtain a high-optical-confinement waveguide structure, the structure requires a low refractive index material to use as cladding layers of the waveguide. To examine a waveguide characteristic of the GaN-based waveguide, however, the GaN waveguide structure was also fabricated and characterized. The fabrication of GaN waveguide was successfully demonstrated by the inductively coupled plasma etching technique. The

new waveguide characterization method, using supercontinuum light source, was proposed and demonstrated for the first time. This characterization method has clarified that the waveguide structure grown by metalorganic vapor phase epitaxy has very good crystalline quality suitable for the fabrication of intersubband transition devices. On the other hand, the waveguide structure grown by molecular beam epitaxy provides a high propagation loss for TM-polarization (the polarization that intersubband absorption exists) owing to a high density of crystalline defects in the structure. It was thus found that in order to fabricate a high-quality waveguide of nitride-based semiconductors, not only the waveguide fabrication process, but also the epitaxial growth of the waveguide structure requires a careful concern of each step to obtain the best quality. In case of the epitaxial growth, it was found that the metalorganic vapor phase epitaxy is needed for the growth of a thick epilayer with high crystalline quality, while the molecular beam epitaxy is also needed for the growth of multiple quantum well structures with intersubband absorption at 1.55 μm. A combination of both the metalorganic vapor phase epitaxy and molecular beam epitaxy is therefore a solution to achieve the waveguides for the realization of intersubband transition devices.

In Chapter 5, the AlN-based waveguide structures were proposed and fabricated. It was found out by simulation that using the AlN as cladding layers can improve the optical confinement of the waveguide. Moreover, the AlN has many advantages for fabrication of intersubband transition devices, for example, good carrier confinement, strong built-in electric field, low refractive index and low reflectance. Three high-optical-confinement waveguide structures were therefore designed and studied for the waveguide fabrication. The epitaxial growth of high crystalline quality AlN was successfully performed with metalorganic vapor phase epitaxy using optimized growth condition. The fabrication of high quality AlN waveguide was demonstrated with low propagation loss. Furthermore, the growth of high-optical-confinement waveguide structure was demonstrated with metalorganic vapor phase epitaxy, and the waveguide was successfully fabricated with the inductively coupled plasma etching technique. The waveguide characterization by supercontinuum light source revealed that the waveguide fabricated by metalorganic vapor phase epitaxial growth with excellent etching technique can provide good waveguide characteristic suitable for the intersubband

transition devices.

In Chapter 6, the fabrication of the intersubband transition device using AlN waveguide with GaN/AlN multiple quantum wells was demonstrated. The growth of the multiple quantum wells on the AlN layer was studied and found that there exists very strong built-in electric field induced in the GaN quantum wells. This built-in electric field is useful for shortening the wavelength of intersubband absorption. By making use of this strong built-in electric field, the waveguide structure with GaN/AlN quantum wells could be fabricated for a certain intersubband absorption wavelength, without wavelength shifting caused by a change in built-in electric field, especially for a wavelength shorter than 1.4 μm. The intersubband absorption at a wavelength as short as 1.3 μm was therefore achieved in the AlN waveguide structure with GaN/AlN quantum wells for the first time.

The intersubband absorption saturation in the device was demonstrated by the pump-probe measurements using ultrashort optical pulse: 7 dB of absorption saturation was observed for input optical-pulse energy of 200 pJ. In addition to the demonstration of intersubband transition device based on AlN waveguide, the wavelength tuning of the device was also demonstrated by changing the quantum well and barrier thicknesses with a careful consideration of the built-in electric field in the quantum wells, leading to the realization of longer wavelength including 1.55 μm. Although it is the first device that can operate in the optical wavelength range of 1.3-1.55 μm, the ultrafast optical-switching characteristic of this AlN-waveguide-based device measured by pump-probe measurements is good, comparable to those of the previously reported GaN-waveguide-based devices. Moreover, the first AlN-waveguide-based ultrafast all-optical switch operating at 1.55 μm was demonstrated by the careful concern of AlN barrier thickness and optical confinement of the waveguide structure. The switch has very good saturable absorption characteristic for 1.55 μm: the smallest input energy of 90 pJ to obtain 10-dB saturation, which is the best characteristic ever reported for nitride-based intersubband-transition ultrafast all-optical switch.

Such achievements were originated from the characteristic of AlN waveguide structure and the successes in fabricating the structure with high quality. With additional improvement of the waveguide structure and a careful wavelength-tuning, the

AlN-waveguide-based device is expected to have much better characteristic for applications on ultrafast all-optical switching. Finally, the parameters that affect the switching energy of the device were discussed. Since the switching energy is inversely dependent on the operating speed, in order to achieve the all-optical switch with ultrafast operating speed, the requirement of optical pulses with high switching energy is inevitable. Nevertheless, the switching energy can be reduced by further improvement of the waveguide structure and waveguide fabrication process to reduce the insertion loss. With the optimization of each process, it is believed that the AlN waveguide structure is a very promising structure that can be used to realize the low switching energy ultrafast all-optical switch operating at a bit rate higher than 5 Tb/s for future photonic networks.

APPENDIX A
Principles of Electronic Band Structure

For an electron in a periodic potential

$$V(\mathbf{r}) = V(\mathbf{r} + \mathbf{R}) \tag{A.1}$$

where $\mathbf{R} = n_1\mathbf{a}_1+n_2\mathbf{a}_2+n_3\mathbf{a}_3$, and $\mathbf{a}_1$, $\mathbf{a}_2$, $\mathbf{a}_3$ are the lattice vectors, and n_1, n_2, n_3 are integers, the electron wave function satisfies the Schrödinger equation [183]

$$H\psi(\mathbf{r}) = \left[\frac{-\hbar^2}{2m_o}\nabla^2 + V(\mathbf{r})\right]\psi(\mathbf{r}) = E(\mathbf{k})\psi(\mathbf{r}) \tag{A.2}$$

The Hamiltonian is invariant under translation by the lattice vectors, $\mathbf{r} \rightarrow \mathbf{r} + \mathbf{R}$. If $\psi_{\mathbf{k}}(\mathbf{r})$ describes an electron moving in the crystal, $\psi_{\mathbf{k}}(\mathbf{r} + \mathbf{R})$ will also be a solution to (A.1). The general solution of the above equation is given by

$$\psi_{n\mathbf{k}}(\mathbf{r}) = u_{n\mathbf{k}}(\mathbf{r})\cdot e^{i\mathbf{k}\cdot\mathbf{r}} \tag{A.3}$$

where $u_{n\mathbf{k}}(\mathbf{r})$ has the period of the crystal lattice with $u_{\mathbf{k}}(\mathbf{r}) = u_{\mathbf{k}}(\mathbf{r}+\mathbf{R})$.
This result is the Bloch theorem. The wave function $\psi_{n\mathbf{k}}(\mathbf{r})$ is usually called the Bloch function. The corresponding energy is given by

$$E = E_n(\mathbf{k}) \tag{A.4}$$

Here n refers to the band and k the wave vector of the electron. The full description of the band structure requires numerical methods. The effective mass theory for the conduction band is obtained from the dispersion relation:

$$E(k) = \frac{\hbar^2 k^2}{2m^*} \tag{A.5}$$

where the effective mass of the electron in the conduction band is $m^* = m_b^*$ in the barrier region and $m^* = m_w^*$ in the quantum well. In the presence of the quantum-well potential,

$$V(z) = \begin{cases} 0 & ,|z| \le \dfrac{L_w}{2} \\ V_0 (= \Delta E_c) & ,|z| > \dfrac{L_w}{2} \end{cases} \tag{A.6}$$

where the energies are all measured from the conduction band edge. The effective mass equation (4.4.5) for a single band is [184]

$$\left[-\frac{\hbar^2}{2} \frac{\partial}{\partial z} \frac{1}{m(z)} \frac{\partial}{\partial z} + \frac{\hbar^2}{2m(z)} \nabla_t^2 + V(z) \right] \psi(r) = E\psi(r) \tag{A.7}$$

In general, the wave function $\psi_{\mathbf{k}}$ can be written in the form

$$\psi(r) = \frac{e^{ik_t \cdot \rho}}{\sqrt{A}} \psi(z) \tag{A.8}$$

and

$$-\frac{\hbar^2}{2} \frac{\partial}{\partial z} \frac{1}{m(z)} \frac{\partial}{\partial z} \psi(z) + V(z)\psi(z) = \left(E(k_t) - \frac{\hbar^2 k_t^2}{2m(z)} \right) \psi(z) \tag{A.9}$$

The eigenvalue and the eigenfunction obtained from the above equation are the Energy level and corresponding wave function of the conduction subband, respectively. Here, we ignore the k_t dependence of ψ(z). Eq. A.9 can be solved at $k_t = 0$ for the n^{th} subband energy $E_n(0)$ with a wave function $\psi(z) = f_n(z)$. Then we have

$$E_n(k_t) = E_n(0) + \frac{\hbar^2 k^2}{2m_w} \tag{A.10}$$

APPENDIX B
Principles of Optical Transition

Consider a semiconductor illuminated by light, the interaction between the photons and the electrons in the semiconductor can be described by the Hamiltonian [185]

$$H = \frac{1}{2m_0}(\mathbf{p} - q\mathbf{A})^2 + V(\mathbf{r}) \tag{B.1}$$

Thus the electron-photon interaction Hamiltonian can be described as

$$\begin{aligned} H &= \frac{\mathbf{p}^2}{2m_0} + V(\mathbf{r}) - \frac{q}{2m_0}(\mathbf{p}\cdot\mathbf{A} + \mathbf{A}\cdot\mathbf{p}) + \frac{q^2\mathbf{A}^2}{2m_0} \\ &\cong H_0 + H' \end{aligned} \tag{B.2}$$

The interaction Hamiltonian can be derived to the relation

$$H' = -\frac{qA_0 e^{i\mathbf{k}_{op}\cdot\mathbf{r}}}{2m_0}\hat{e}\cdot\mathbf{p} \tag{B.3}$$

where $\mathbf{k}_{op}$ is the wave vector and $\hat{e}$ is a unit vector in the direction of the optical electric field. With the interaction above, the transition rate for the absorption of a photon, assuming an electron is initially at state E_a, is given by Fermi's golden rule and treated with the time-dependent perturbation theory, can be written as

$$W_{abs} = \frac{2\pi}{\hbar}\left|\langle b|H'(\mathbf{r})|a\rangle\right|^2 \delta(E_b - E_a - \hbar\omega) \tag{B.4}$$

where $E_b > E_a$.

Similarly the transition rate for the emission of a photon if an electron is initially at state E_b is

$$W_{\text{ems}} = \frac{2\pi}{\hbar}\left|\langle a|H'(\mathbf{r})|b\rangle\right|^2 \delta(E_a - E_b + \hbar\omega) \tag{B.5}$$

The total upward transition rate per unit volume ($s^{-1}cm^{-3}$) in the crystal is

$$R_{a\to b} = \frac{2}{V}\sum_{\mathbf{k}_a}\sum_{\mathbf{k}_b}\frac{2\pi}{\hbar}\left|H'_{ba}\right|^2 \delta(E_a - E_b + \hbar\omega) f_a(1-f_b) \tag{B.6}$$

where the probability of the occupied state a is assumed as the Fermi-Dirac distribution.

$$f_a = \frac{1}{1+e^{(E_a - E_F)/k_B T}} \tag{B.7}$$

With the similar treatment, the rate of the downward transition rate per unit volume, with aid of $|H'_{ba}| = |H'_{ab}|$, can be written as

$$R_{b\to a} = \frac{2}{V}\sum_{\mathbf{k}_a}\sum_{\mathbf{k}_b}\frac{2\pi}{\hbar}\left|H'_{ba}\right|^2 \delta(E_a - E_b + \hbar\omega) f_b(1-f_a) \tag{B.8}$$

Thus, the net upward transition rate per unit volumn can be written as

$$\begin{aligned} R &= R_{a\to b} - R_{b\to a} \\ &= \frac{2}{V}\sum_{\mathbf{k}_a}\sum_{\mathbf{k}_b}\frac{2\pi}{\hbar}\left|H'_{ba}\right|^2 \delta(E_b - E_a - \hbar\omega)(f_a - f_b) \end{aligned} \tag{B.9}$$

Then, with the definition of the absorption coefficient, Eq. A.19 can be derived as follows.

$$\begin{aligned}\alpha &= \frac{\text{No. of photons absorbed per unit volume per second}}{\text{No. of photons injected per unit area per second}} \\ &= \frac{\mathrm{R}}{(\mathrm{S}/\hbar\omega)} \\ &= \frac{\hbar\omega}{(n_r\omega^2 A_0^2/2\mu c)}\frac{2}{V}\sum_{\mathbf{k}_a}\sum_{\mathbf{k}_b}\frac{2\pi}{\hbar}|H'_{ba}|^2\delta(E_b - E_a - \hbar\omega)(f_a - f_b)\end{aligned} \tag{B.10}$$

Using the dipole approximation that $\mathbf{A}(\mathbf{r}) = \mathbf{A}e^{i\mathbf{k}_{op}\cdot\mathbf{r}} \cong \mathbf{A}$, we can write

$$H'_{ba} = -\frac{q}{m_0}\mathbf{A}\cdot\langle b|\mathbf{p}|a\rangle = -\frac{qA_0}{2m_0}\hat{e}\cdot\mathbf{p}_{ba} \tag{B.11}$$

The absorption coefficient in Eq. B.10 then becomes

$$\alpha(\hbar\omega) = \frac{\pi q^2}{n_r c\varepsilon_0 m_0^2\omega}\frac{2}{V}\sum_{\mathbf{k}_a}\sum_{\mathbf{k}_b}\frac{2\pi}{\hbar}|\hat{e}\cdot\mathbf{p}_{ba}|^2\delta(E_b - E_a - \hbar\omega)(f_a - f_b) \tag{B.12}$$

The Hamiltonian can also be written in terms of the electric dipole moment:

$$\boldsymbol{\mu}_{ba} = e\langle b|\mathbf{r}|a\rangle = e\mathbf{r}_{ba} \tag{B.13}$$

$$H'_{ba} = -\langle b|e\mathbf{r}\cdot\mathbf{E}|a\rangle = -\boldsymbol{\mu}_{ba}\cdot\mathbf{E} \tag{B.14}$$

And we can write the absorption coefficient in terms of the dipole moment as

$$\alpha(\hbar\omega) = \frac{\pi\omega}{n_r c\varepsilon_0}\frac{2}{V}\sum_{k_a}\sum_{k_b}|\hat{e}\cdot\boldsymbol{\mu}_{ba}|^2\delta(E_b - E_a - \hbar\omega)(f_a - f_b) \tag{B.15}$$

The delta function may be replaced by a Lorentzian function with a linewidth Γ:

$$\delta(E_b - E_a - \hbar\omega) \rightarrow \frac{\Gamma/(2\pi)}{(E_b - E_a - \hbar\omega)^2 + \Gamma/(2)^2} \tag{B.16}$$

APPENDIX C
Principles of Intersubband Absorption

Consider the intersubband transition between the ground state,

$$\psi_a(\mathbf{r}) = u_c(\mathbf{r})\frac{e^{i\mathbf{k}_t\cdot\boldsymbol{\rho}}}{\sqrt{A}}\phi_1(z) \tag{C.1}$$

and the first excited state, $$\psi_b(\mathbf{r}) = u_{c'}(\mathbf{r})\frac{e^{i\mathbf{k}'_t\cdot\boldsymbol{\rho}}}{\sqrt{A}}\phi_2(z) \tag{C.2}$$

where the transverse wave vectors $\mathbf{k}_t = k_x\hat{x} + k_y\hat{y}$, $\mathbf{k}'_t = k'_x\hat{x} + k'_y\hat{y}$ and the position vector $\boldsymbol{\rho} = x\hat{x} + y\hat{y}$ in the quantum-well plane have been used. The optical dipole moment is given by [186]

$$\begin{aligned}\boldsymbol{\mu}_{ba} &= \langle\psi_b|e\mathbf{r}|\psi_a\rangle \\ &\simeq \langle u_c|u_{c'}\rangle\left\langle\frac{e^{i\mathbf{k}'_t\cdot\boldsymbol{\rho}}}{\sqrt{A}}\phi_2|e\mathbf{r}|\frac{e^{i\mathbf{k}_t\cdot\boldsymbol{\rho}}}{\sqrt{A}}\phi_1\right\rangle \\ &\simeq \delta_{\mathbf{k}_t,\mathbf{k}'_c}\langle\phi_2|ez|\phi_1\rangle\hat{z}\end{aligned} \tag{C.3}$$

which has only a z component, where the orthonormal conditions, $\langle\phi_1|\phi_2\rangle = 0$ and $\langle u_c|u_{c'}\rangle \simeq 1$, are used.

Let consider the transition between two subband energies, which the initial state and the final states are, respectively,

$$\begin{aligned}E_a &= E_1 + \frac{\hbar^2 k^2{}_t}{2m_e^*} \\ E_b &= E_2 + \frac{\hbar^2 k^2{}_t}{2m_e^*}\end{aligned} \tag{C.4}$$

Since the x and y components of the intersubband dipole moment in Eq. C.3 are zero, we obtain nonzero absorption coefficient only for $\hat{e} = \hat{z}$. This is the reason why only TM polarization is allowed for the intersubband absorption.

The absorption coefficient can be derived as follows.

$$\begin{aligned}
\alpha(\hbar\omega) &= \left(\frac{\omega}{n_r c\varepsilon_0}\right)\frac{2}{V}\sum_{\mathbf{k}_t}\sum_{\mathbf{k}_t'}\frac{\left|\hat{e}\cdot\mu_{ba}\right|^2(\Gamma/2)}{(E_b - E_a - \hbar\omega)^2 + (\Gamma/2)^2}(f_a - f_b) \\
&= \left(\frac{\omega}{n_r c\varepsilon_0}\right)\frac{2}{V}\sum_{\mathbf{k}_t}\frac{\left|\mu_{21}\right|^2(\Gamma/2)}{(E_2 - E_1 - \hbar\omega)^2 + (\Gamma/2)^2}(f_a - f_b) \qquad \text{(C.5)} \\
&= \left(\frac{\omega}{n_r c\varepsilon_0}\right)\frac{\left|\mu_{21}\right|^2(\Gamma/2)}{(E_2 - E_1 - \hbar\omega)^2 + (\Gamma/2)^2}(N_a - N_b)
\end{aligned}$$

where $\mu_{21} = \langle\phi_2|ez|\phi_1\rangle = \int\phi_2^*(z)ez\phi_1(z)dz$ is the intersubband dipole moment, and N_i is the number of electrons per unit volume in the ith subband, which is given as

$$N_i = \frac{m_e^* k_B T}{\pi\hbar^2 L_z}\ln\left(1 + e^{(E_F - E_i)/k_B T}\right) \qquad \text{(C.6)}$$

The absorption coefficient is, therefore,

$$\alpha(\hbar\omega) = \left(\frac{\omega}{n_r c\varepsilon_0}\right)\frac{\left|\mu_{21}\right|^2(\Gamma/2)}{(E_2 - E_1 - \hbar\omega)^2 + (\Gamma/2)^2}\left(\frac{m_e^* k_B T}{\pi\hbar^2 L}\right)\ln\left(\frac{1 + e^{(E_F - E_1)/k_B T}}{1 + e^{(E_F - E_2)/k_B T}}\right) \qquad \text{(C.7)}$$

which is a Lorentzian shape with a linewidth Γ.

APPENDIX D
Calculation of Built-in Electric-Field Effect

For GaN/AlN multiple quantum well structures, an important parameter that affects the intersubband transition energy is the built-in electric field. This electric field is induced mostly by stress in the quantum wells through the piezoelectric effect [187]. In addition, the built-in electric field is strengthened by the spontaneous polarization, which has very strong effect in wurtzite group-III nitrides [188]. The total electric field induced by both piezoelectric and spontaneous polarization can bend the band structure of the quantum wells to be inclined with a slope, thus changing the effective barrier height and the wave function of each subband energy level.

To study the effect of this built-in electric field, the dependence of electric field in the quantum wells on the subband energy is calculated in Fig. D.1 In this calculation, the electric field strength is assumed to be constant throughout the quantum well and the also the barrier. The summation of the potential is due to the electric field is assumed to be equal to zero for each pair of GaN quantum well and AlN barrier. Clearly it can be

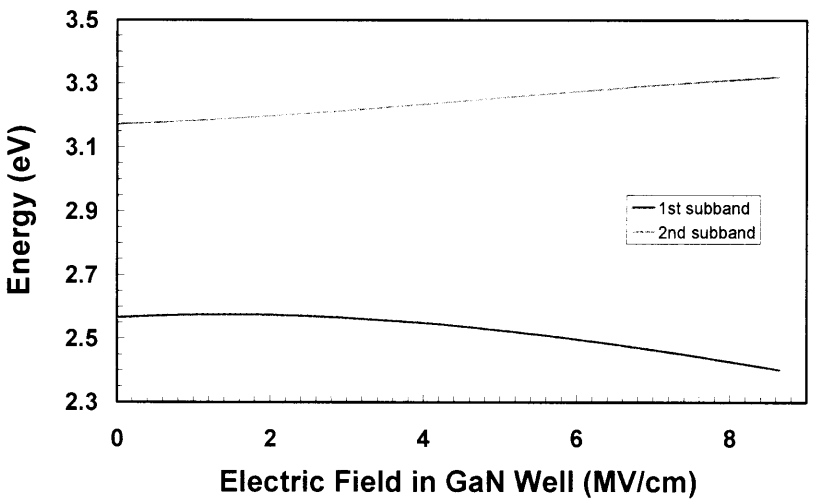

Figure D.1 1st and 2nd subband energy levels in a GaN/AlN quantum well plotted as a function of electric field in 2-nm-thick GaN well

seen that with increasing electric field, the 1st subband energy level shifts to lower energy side, whereas the 2nd subband energy level shifts to higher energy side. This shifting causes larger difference of energy between 1st and 2nd subband energy levels, resulting in larger intersubband transition energy. In other words, the intersubband transition energy increases with strength of built-in electric field. This effect therefore helps making a blue shift of intersubband transition wavelength.

Fig. D.2 shows the calculation results for the intersubband transition wavelength dependence on the well thickness with different built-in electric-field strength in the GaN/AlN multiple quantum wells. The results confirm that the built-in field has a great effect to cause a blue shift of the intersubband transition wavelength. When the quantum well is thicker than 2.0 nm, the intersubband transition wavelength can shift to shorter wavelength with a wide range depending on the strength of the built-in electric field. Nevertheless, with the quantum well thinner than 1.5 nm, the effect of the built-in electric field becomes almost negligible and can be approximated as a flat-band condition in which the built-in electric field are not taking into account (0 MV/cm). This is because when the well is very thin, the slope of inclining of the band structure does not have much influence on the energy level of each subband, resulting in no changes of the transition energy.

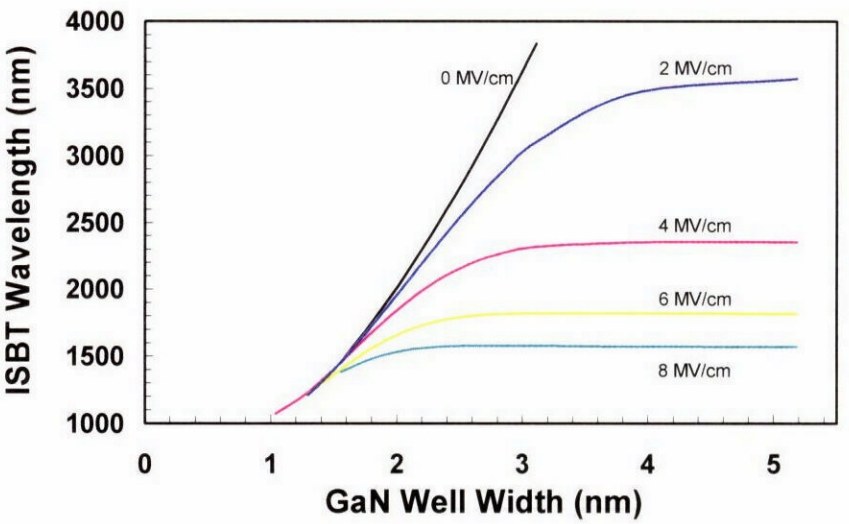

Figure D.2 Wavelength of intersubband transition in a GaN/AlN MQW structure with different well widths calculated by taking into account the built-in electric field: (a) 0 MV/cm, (b) 2 MV/cm, (3) 4 MV/cm, (4) 6 MV/cm, (5) 8 MV/cm

REFERENCES

[1] M. Suzuki, H. Tanaka, N. Edagawa, K. Utaka, and Y Matsushima, "Transform-limited Optical pulse Generation up to 20-GHz Repetition Rate by a Sinusoidally Driven InGaAsP Electroabsorption Modulator," *IEEE J. Lightwave Technol.* **11**, 468-473 (1993).

[2] P. S. Cho, D. Mahgerefteh, J. Goldhar, "All-optical 2R regeneration and wavelength conversion at 20 Gb/s using an electroabsorption modulator," *IEEE Photon. Technol. Lett.* **11**, 1662-1664 (1999).

[3] P. S. Cho, et al., "All-optical regeneration at the receiver of 10-Gb/s RZ data transmitted over 30 000 km using an electroabsorption modulator," *IEEE Photon. Technol. Lett.* **12**, 205-207 (2000).

[4] E. S. Awad, et al. "Optical 3R regeneration using a single EAM for all-optical timing extraction with simultaneous reshaping and wavelength conversion," *IEEE Photon. Technol. Lett.* **14**, 1378-1380 (2002).

[5] K. K. Chow, C. Shu, "All-optical wavelength conversion with multicasting at 6 x 10 Gbit/s using electroabsorption modulator," *Electron. Lett.* **39**, 1395-1397 (2003).

[6] E.S. Awad, P. Cho, J. Goldhar, "High-speed all-optical and gate using nonlinear transmission of electroabsorption modulator," *IEEE Photon. Technol. Lett.* **13**, 472-474 (2001).

[7] K. Tajima, "All-optical Switch with Switch-off Time Unrestricted by Carrier Lifetime," *Jpn. J. Appl. Phys.* Part 2 **32**, L1746-L1749 (1993).

[8] C. Schubert, S. Diez, J. Berger, R. Ludwig, U. Feiste, H. G. Weber, G. Toptchiyski, and K. Petermann, "160-Gbit/s all-optical demultiplexing using a gain-transparent ultrafast-nonlinear interferometer (GT-Uni)," *IEEE Photon. Technol. Lett.* **13**, 475-477 (2001).

[9] S. Nakamura, Y. Ueno, K. Tajima, J. Sasaki, T. Sugimoto, T. Kato, T. Shimoda, M. Itoh, H. Hatakeyama, T. Tamanuki, and T. Sasaki, "Demultiplexing of 168-Gb/s data pulses with a hybrid-integrated symmetric Mach-Zehnder all-optical switch," *IEEE Photon. Technol. Lett.* **12**, 425-427 (2000).

[10] S. Diez, R. Ludwig, and H. G. Weber, "Gain-transparent SOA-switch for highbitrate OTDM add/drop multiplexing," *IEEE Photon. Technol. Lett.* **11**, 60-62 (1999).

[11] St. Fischer, M. Duelk, M. Puleo, R. Girardi, E. Gamper, W. Vogt, W. Hunziker, E. Gini, and H. Melchior, "40-Gb/s OTDM to 4 WDM conversion in monolithic InP Mach-Zehnder interferometer module," *IEEE Photon. Technol. Lett.* **11**, 1262-1264 (1999).

[12] Tsurusawa M, Nishimura K, Usami M, "First demonstration of simultaneous demultiplexing from 40 Gbit/s into two channels of 20 Gbit/s by SOA-based alloptical polarisation switch," *Electron. Lett.* **37**, 1398-1399 (2001).

[13] S. Nakamura, Y. Ueno, and K. Tajima, "Error-free all-optical demultiplexing at 336 Gb/s with a hybrid integrated Symmetric-Mach-Zehnder switch," Optical Fiber Communication Conference *(OFC 2002)*, Postdeadline Paper FD3 (2002).

[14] J. Leuthold, et al. "All-optical Mach-Zehnder interferometer wavelength converters and switches with intergrated data- and control-signal separation scheme", *IEEE J. Lightwave Technol.* **17**, 1056-1066 (1999).

[15] J. Leuthold, et al. "All-optical space switches with gain and principally ideal extinction ratios", *IEEE J. Quantum Electron.* **34**, 622-633 (1998).

[16] J. Leuthold, et al. "Multimode Interference Couplers for the Conversion and Combinig of Zero- and First-Order Modes", *IEEE J. Lightwave Technol.* **16**, 1228-1239 (1998).

[17] B. Mikkelsen, K.S. Jepsen, M. Vaa, H.N. Poulsen, K.E. Stubkjaer, R. Hess, M. Duelk, W. Vogt, E. Gamper, E. Gini, P.A. Besse, H. Melchior, S. Bouchoule, F. Devaux, "All-optical wavelength converter scheme for high speed RZ signal formats," *Electron. Lett.* **33**, 2137-2139 (1997).

[18] S. Nakamura, Y. Ueno, K. Tajima, "168-Gb/s all-optical wavelength conversion with a Symmetric-Mach-Xehnder-type switch," *IEEE Photon. Technol. Lett.* **13**, 1091-1093 (2001).

[19] J. Leuthold, et al., "100 Gbit/s all-optical wavelength conversion with integrated SOA delayed-interference configuration," *Electron. Lett.* **36**, 1129-1130 (2000).

[20] J. Leuthold, et al., "All-optical wavelength conversion between 10 and 100 Gb/s with SOA delayed-interference configuration," *Opt. Quantum Electron.* **33**,

939-952 (2001).

[21] K. J. Blow, N. J. Doran, and B. P. Nelson, "Demonstration of the nonlinear fibre loop mirror as an ultrafast all-optical demultiplexer," *Electron. Lett.* **26**, 962-964, (1990).

[22] M. Jinno and T. Matsumoto, "Ultrafast low-power and highly stable fiber Sagnac interferometer," *IEEE Photon. Technol. Lett.* **2**, 349-351 (1990).

[23] T. Yamamoto, E. Yoshida, and M. Nakazawa, "Ultrafast nonlinear optical loop mirror for demultiplexing 640 Gbit/s TDM signals," *Electron. Lett.* **34**, 1013-1014 (1998).

[24] M. Nakazawa, T. Yamamoto, and K. R. Tamura, "1.28 Tbit/s-70 km OTDM transmission using third and fourth-order simultaneous dispersion compensation with a phase modulator," *Electron. Lett.* **36**, 2027-2029 (2000).

[25] J. Yu, Y. Qian, A.T. Clausen, H.N. Poulsen, P. Jeppesen, and S.N. Knudsen, "40Gbit/s pulsewidth-maintained wavelength conversion based on a high-nonlinearity," *Electron. Lett.* **36**, 1633-1635 (2000).

[26] H. Sotobayashi, et al. "Ultrafast walk-off-free nonlinear optical loop mirror by a simplified configuration for 320-Gbit/s time-division multiplexing signal demultiplexing," *Opt. Lett.* **27**, 1555-1557 (2002).

[27] T. Morioka, S. Kawanishi, H. Takara, and M. Saruwatari, "Multiple output 100 Gbit/s all-optical demultiplexer based on multichannel four-wave mixing pumped by a linearly-chirped square pulse," *Electron. Lett.* **30**, 1959-1960 (1994).

[28] T. Morioka, H. Takara, S. Kawanishi, T. Kitoh, and M. Saruwatari, "Error-free 500 Gbit/s all-optical demultiplexing using low-noise, low-jitter supercontinuum short pulses," *Electron. Lett.* **32**, 833-834 (1996).

[29] H. Sotobayashi, W. Chujo, T. Ozeki, "80Gbit/s simultaneous photonic demultiplexing based on OTDM-to-WDM conversion by four-wave mixing with supercontinuum light source," *Electron. Lett.* **37**, 640-642 (2001).

[30] L.C. West and S.J. Eglash, "First observation of an extremely large-dipole infrared transition within the conduction band of a GaAs quantum well," *Appl. Phys. Lett.* **46**, 1156-1158 (1985).

[31] B. F. Levine, R. J. Malik, J. Walker, K. K. Choi, C. G. Bethea, D. A. Kleinman, J. Vandenberg, "Strong 8.2 μm infrared intersubband absorption in doped

GaAs/AlAs quantum well waveguides," *Appl. Phys. Lett.* **50**, 273-275 (1987).

[32] A. Harwitt and J. S. Harris, "Observation of Stark shifts in quantum well intersubband transitions," *Appl. Phys. Lett.* **50**, 685-687 (1987).

[33] H. C. Liu, F. Capasso, *Intersubband Transitions in Quantum Wells: Physics and Device Applications I* (Academic Press, San Diego, 2000) Semiconductors and Semimetals Vol.62.

[34] H. C. Liu, F. Capasso, *Intersubband Transitions in Quantum Wells: Physics and Device Applications II* (Academic Press, San Diego, 2000) Semiconductors and Semimetals Vol.66.

[35] B. K. Ridley, "Theoretical model for polarization superlattices: Energy levels and intersubband transitions," *J. Appl. Phys.* **94**, 3972-3978 (2003).

[36] B. F. Levine, K. K. Choi, C. G. Bethea, J. Walker, and R. J. Malik, "New 10 μm infrared detector using intersubband absorption in resonant tunneling GaAlAs superlattices", *Appl. Phys. Lett.* **50**, 1092-1094 (1987).

[37] B. F. Levine, "Quantum-well infrared photodetectors", *J. Appl. Phys.* **74**, R1-R81 (1993).

[38] S. D. Gunapala, J. S. Park, G. Sarusi, T. Lin, J. K. Liu, P. D. Maker, R. E. Muller, C. A.Shott, and T. Hoelter, "15-μm 128 x 128 GaAs/$Al_xGa_{1-x}As$ Quantum Well Infrared Photodetector Focal Plane Array Camera," *IEEE Trans. Electron. Devices* **44**, 45-50 (1997).

[39] A. Majumdar, K. K. Choi, J. L. Reno, L. P. Rokhinson and D. C. Tsui, "Two-color quantum-well infrared photodetector with voltage tunable peaks," *Appl. Phys. Lett.* **80**, 707-709 (2002).

[40] A. Rogalski, "Quantum well photoconductors in infrared detector technology," *J. Appl. Phys.* **93**, 4355-4391 (2003).

[41] D. Hofstetter, S.-S. Schad, H. Wu, W. J. Schaff, and L. F. Eastman, "GaN/AlN-based quantum well infrared photodetector for 1.55 μm," *Appl. Phys. Lett.* **83**, 572-574 (2003).

[42] J. Faist, F. Capasso, D. L. Sivco, C. Sirtori, A. L. Hutchinson, A. Y. Cho, "Quantum cascade lasers," *Science* **264**, 553 (1994).

[43] J. Faist, F. Capasso, C. Sirtori, D. L. Sivco, A. L. Hutchinson, and A. Y. Cho, "Vertical transition quantum cascade laser with Bragg confined excited state,"

Appl. Phys. Lett. **66**, 538 (1995).

[44] J. Faist, F. Capasso, C. Sirtori, D. L. Sivco, A. L. Hutchinson, and A. Y. Cho, "Continuous wave operation of a vertical transition quantum cascade laser above *T*=80 K," *Appl. Phys. Lett.* **67**, 3057 (1995).

[45] F. Capasso, A. Tredicucci, C. Gmachl, D. L. Sivco, A. L. Hutchinson, A. Y. Cho, and G. Scamarcio, "High-Performance Superlattice Quantum Cascade lasers," *IEEE J. Select. Topic Quantum Electron.* **5**, 792 (1995).

[46] A. Tredicucci, F. Capasso, C. Gmachl, D. L. Sivco, A. L. Hutchinson, and A. Y. Cho, "High performance interminiband quantum cascade lasers with graded superlattices," *Appl. Phys. Lett.* **73**, 2101-2103 (1998).

[47] O. Gauthier-Lafaye, F. H. Julien, S. Cabaret, J. M. Lourtioz, G. Strasser, E. Gornik, M. Helm, and P. Bois, "High-power GaAs/AlGaAs Quantum Fountain Unipolar Laser emitting at 14.5 μm with 2.5% tunability," *Appl. Phys. Lett.* **74**, 1537 (1999).

[48] S. A. Lynch, et al, "Intersubband electroluminescense from Si/SiGe cascade emitters at terahertz frequencies," *Appl. Phys. Lett.* **81**, 1543-1545 (2002).

[49] R. Kohler, A. Tredicucci, F. Beltram, H. E. Beere, E. H. Linfield, A. G. Davies and D. A. Ritchie, "Low-threshold quantum cascade lasers at 3.5 THz (λ = 85 μm)," *Opt. Lett.* **28**, 810-813 (2003).

[50] J. S. Roberts, et al, "Quantum cascade lasers grown by metalorganic vapor phase epitaxy," *Appl. Phys. Lett.* **82**, 4221-4223 (2003).

[51] R. P. Green, et al, "Room-temperature operation of InGaAs/AlInAs quantum cascade lasers grown by metalorganic vapor phase epitaxy," *Appl. Phys. Lett.* **83**, 1921-1923 (2003).

[52] D.G. Revin et al, "$\lambda \sim$ 4−5.3 μm intersubband emission from InGaAs-AlAsSb quantum cascade structures," *Appl. Phys. Lett.* **84**, 1447-1449 (2004).

[53] A. Neogi, H. Yoshida, T. Mozume, and O. Wada, "Ultrafast all-optical modulation of interband-light pulses by ultrashort intersubband light pulses in semiconductor quantum wells," *J. Appl. Phys.* **85**, 3352-3358 (1999).

[54] H. Yoshida, T. Mozume, A. Neogi, and O. Wada, "Ultrafast all-optical switching at 1.3μm/1.55μm using InGaAs/AlAsSb/InP coupled double quantum well structure for intersubband transitions," *Electron. Lett.* **35**, 1103-1105 (1999).

[55] T. Asano, M. Tamura, S. Yoshizawa and S. Noda, "Pump-probe measurement of ultrafast all-optical modulation based on intersubband transition in n-doped quantum wells," *Appl. Phys. Lett.* **77**, 19-21 (2000).

[56] A.V. Gopal, H. Yoshida, A. Neogi, T. Mozume, N. Georgiev, O. Wada, and H. Ishikawa, "Absorption saturation of intersubband transition in InGaAs/AlAsSb quantum well characterized by absorption spectral analysis," *Jpn. J. Appl. Phys.* **40**, L1015-L1018 (2001).

[57] A. V. Gopal, H. Yoshida, A. Neogi, T. Mozume, N. Georgiev, T. Simoyama, O. Wada, and H. Ishikawa, "Large improvement in intersubband saturation intensity in InGaAs/AlAsSb quantum well," *Electron. Lett.* **37**, 1265-1267 (2001).

[58] T. Akiyama, N. Georgiev, T. Mozume, H. Yoshida, A.V. Gopal, and O. Wada, "1.55 mm picosecond all-optical switching by using intersubband absorption in InGaAs-AlAs-AlAsSb coupled quantum wells," *IEEE Photon. Technol. Lett.* **14**, 495-497 (2002).

[59] T. Mozume, J. Kasai, N. Georgiev, T. Simoyama, V. Achanta and H. Yoshida, "Ultralow Intersubband Absorption Saturation Intensity at Communication Wavelength Achieved in Novel Strain Compensated InGaAs/AlAs/AlAsSb Quantum Wells Grown by Molecular Beam Epitaxy," *Jpn. J. Appl. Phys.* **42**, 5500-5507 (2003).

[60] T. Simoyama, H. Yoshida, J. Kasai, T. Mozume, A. V. Gopal and H. Ishikawa, "InGaAs-AlAs-AlAsSb coupled quantum well intersubband transition all-optical switch with low switching energy for OTDM systems," *IEEE Photon. Technol. Lett.* **15**, 1363-1365 (2003).

[61] N. Iizuka, K. Kaneko, and N. Suzuki, "Sub-picosecond modulation by intersubband transition in ridge waveguide with GaN/AlN quantum wells," *Electron. Lett.* **40**, 962-963 (2004).

[62] N. Iizuka, K. Kaneko, and N. Suzuki, "Sub-picosecond all-optical gate utilizing GaN intersubband transition," *Opt. Express* **13**, 3835-3840 (2005).

[63] R. Akimoto, K. Akita, F. Sasaki, T. Hasama, "Sub-picosecond electron relaxation of near-infrared intersubband transitions in n-doped (CdS/ZnSe)/BeTe quantum wells", *Appl. Phys. Lett.* **81**, 2998-3000 (2002).

[64] R. Akimoto, B. Li, K. Akita, T. Hasama, "Ultrafast switching of intersubband

saturable absorber in II-VI-based quantum well waveguides," *32nd European Conference and Exhibition on Optical Communication Conference (ECOC' 2005) Proceedings* **4**, Th 1.6.4, 837-838 (2005).

[65] S. Noda, T. Yamamoto, M. Ohya, Y. Muramoto, and A. Sasaki, "All-optical modulation for semiconductor lasers by using three energy levels in n-doped quantum wells," *IEEE J. Quantum Electron.* **29**, 1640-1647 (1993).

[66] T. Asano and S. Noda, "Relaxation time of short wavelength intersubband transition in InGaAs/AlAs quantum wells," *Jpn. J. Appl. Phys.* **37**, 6020-6024 (1998).

[67] N. Suzuki and N. Iizuka, "Electron Scattering Rates in AlGaN/GaN Quantum Wells for 1.55-μm Inter-subband Transition," *Jpn. J. Appl. Phys.* **37**, L369-L371 (1998).

[68] R. A. Kaindl, et al, "Ultrafast dephasing of coherent intersubband polarizations in a quasi-two-dimensional electron plasma", *Phys. Rev. Lett.* **80**, 3575-3578 (1998).

[69] T. Akiyama, N. Georgiev, T. Mozume, H. Yoshida, A.V. Gopal, and O. Wada, "Nonlinearity and recovery time of 1.55 μm intersubband absorption in InGaAs/AlAs/AlAsSb coupled quantum wells," *Electron. Lett.* **37**, 129-130 (2001).

[70] A. V. Gopal, H. Yoshida, T. Simoyama, J. Kasai, T. Mozume, and H. Ishikawa, "Room-temperature dephasing time of intersubband transitions in heavily-doped InGaAs/AlAs/AlAsSb coupled quantum wells," *Appl. Phys. Lett.* **83**, 1854-1856 (2003).

[71] N. Iizuka, K. Kaneko, N. Suzuki, T. Asano, S. Noda, and O. Wada, "Ultrafast intersubband relaxation (≤ 150 fs) in AlGaN/GaN multiple quantum wells," *Appl. Phys. Lett.* **77**, 648-650 (2000).

[72] C. Gmachl, S. V. Frolov, H. M. Ng, S.-N. G. Chu, and A. Y. Cho, "Sub-picosecond electron scattering time for λ~1.55 μm intersubband transition in GaN/AlGaN multiple quantum wells," *Electron. Lett.* **37**, 378-379 (2001).

[73] J. D. Heber, C. Gmachl, H. M. Ng, and A. Y. Cho, "Comparative study of ultrafast intersubband electron scattering times at ~1.55 μm wavelength in GaN/AlGaN heterostructures," *Appl. Phys. Lett.* **81**, 1237-1239 (2002).

[74] J. Hamazaki, S. Matsui, H. Kunugita, K. Ema, H. Kanazawa, T. Tachibana, A.

Kikuchi, and K. Kishino, "Ultrafast Intersubband Relaxation and Nonlinear Susceptibility at 1.55 μm in GaN/AlN Quantum Wells," *Appl. Phys. Lett.* **84**, 1102-1104 (2004).

[75] J. Hamazaki, H. Kunugita, K. Ema, H. Kanazawa, S. Matsui, Y. Ishii, T. Morita, A. Kikuchi, and K. Kishino, "Ultrafast Intersubband Relaxation and Carrier Cooling in GaN/AlN Quantum Wells," *Ultrafast Phenomena* **XIV**, Springer, 295-297 (2005).

[76] J. Hamazaki, H. Kunugita, K. Ema, A. Kikuchi, and K. Kishino, "Intersubband relaxation dynamics in GaN/AlN multiple quantum wells studied by two-color pump-probe experiments," Phys. Rev. B **71**, 165334 (2005).

[77] B. Sung, H. C. Chui, M. M. Fejer and J. S. Harris, "Near-infrared wavelength intersubband transitions in. high indium content InGaAs/AlAs quantum wells grown on.GaAs," *Electron. Lett.* **33**, 818-820 (1997).

[78] G. Ghislotti, E. Riedo, D. Lelmini, and M. Martinelli, "Intersubband relaxation time for InGaAs/AlAs quantum wells with a large transition energy," *Appl. Phys. Lett.* **75**, 3626-3628 (1999).

[79] T. Mozume, H. Yoshida, A. Neogi, and M. Kudo, "1.45 μm Intersubband Absorption in InGaAs/AlAsSb Grown by Molecular Beam Epitaxy," *Jpn. J. Appl. Phys.* **38**, 1286-1289 (1999).

[80] A. Neogi, T. Mozume, H. Yoshida and O. Wada, "Intersubband transition at 1.3 and 1.55 μm in a novel coupled InGaAs/AlAsSb double-quantum-well structure," *IEEE Photon. Technol. Lett.* **11**, 632 (1999).

[81] N. Suzuki and N. Iizuka, "Effect of Polarization Field on Intersubband Transition in AlGaN/GaN Quantum Wells," *Jpn. J. Appl. Phys.* **38**, L363-L365, 1999.

[82] K. Hoshino, T. Someya, K. Hirakawa, and Y. Arakawa, "Observation of intersubband transition from the first to the third subband (e1-e3) in GaN/AlGaN quantum wells," *phys. stat. sol.* (a) **192**, 27-32 (2002).

[83] I. Waki, C. Kumtornkittikul, Y. Shimogaki, and Y. Nakano, "Shortest intersubband transition wavelength (1.68 μm) achieved in AlN/GaN multiple quantum wells by metalorganic vapor phase epitaxy," *Appl. Phys. Lett.* **82**, 4465-4467 (2003), and Errata, *Appl. Phys. Lett.* **84**, 3703 (2004).

[84] C. Gmachl, H. M. Ng, S.-N. G.. Chu, and A. Y. Cho," Intersubband absorption in

GaN/AlGaN multiple quantum wells in the wavelength range of $\lambda \sim 1.75$-4.2 μm," *Appl. Phys. Lett.* **77**, 334-336 (2000).

[85] C. Gmachl, H. M. Ng, S.-N. G.. Chu, and A.Y. Cho, "Intersubband absorption at ~1.55 μm in well- and modulation-doped GaN/AlGaN multiple quantum wells with superlattice barriers," *Appl. Phys. Lett.* **77**, 3722-3724 (2000).

[86] H. M. Ng, C. Gmachl, S.-N. G.. Chu, and A. Y. Cho, "Molecular beam epitaxy of GaN/AlGaN superlattices for 1.52-4.2 μm intersubband transitions," *J. Crystal Growth* **220**, 432-438 (2000).

[87] C. Gmachl, H. M. Ng, and A. Y. Cho, "Intersubband absorption in degenerately doped GaN/$Al_xGa_{1-x}N$ coupled double quantum wells," *Appl. Phys. Lett.* **79**, 1590-1592 (2001).

[88] K. Kishino, A. Kikuchi, H. Kanazawa, and T. Tachibana, "Intersubband transition in $(GaN)_m/(AlN)_n$ superlattices in the wavelength range from 1.08 to 1.61 μm," *Appl. Phys. Lett.* **81**, 1234-1236 (2002).

[89] N. Iizuka, K. Kaneko, and N. Suzuki, "Near-infrared intersubband absorption in GaN/AlN quantum wells grown by molecular beam epitaxy," *Appl. Phys. Lett.* **81**, 1803-1805 (2002).

[90] A. Helman, et al, "Intersubband spectroscopy of doped and undoped GaN/AlN quantum wells grown by molecular-beam epitaxy," *Appl. Phys. Lett.* **83**, 5196-5198 (2003).

[91] Kh. Moumanis, et al, "Intraband absorptions in GaN/AlN quantum dots in the wavelength range of 1.27-2.4 μm," *Appl. Phys. Lett.* **82**, 868-870 (2003).

[92] D. Hofstetter, et al, "Midinfrared intersubband absorption on AlGaN/GaN-based high-electron-mobility transistors," *Appl. Phys. Lett.* **80**, 2991-2993 (2002).

[93] Q. Zhou, et al, "Infrared optical absorbance of intersubband transitions in GaN/AlGaN multiple quantum well structures," *J. Appl. Phys.* **93**, 10140-10142 (2003).

[94] R. Akimoto, Y. Kinpara, K. Akita, F. Sasaki, and S. Kobayashi, "Short-wavelength intersubband transitions down to 1.6 μm in ZnSe/BeTe type-II superlattices," *Appl. Phys. Lett.* **78**, 580-582 (2001).

[95] R. Akimoto, K. Akita, F. Sasaki, and S. Kobayashi, "Short-wavelength ($\lambda < 2$ μm) intersubband absorption dynamics in ZnSe/BeTe quantum wells," *Appl. Phys. Lett.*

80, 2433-2435 (2002).

[96] R. Akimoto, B. S. Li, K. Akita, and T. Hasama, "Intersubband transition based on a novel II-VI quantum well structure for ultrafast all-optical switching", *Jpn. J. Appl. Phys.* **43**, 1973-1977 (2004).

[97] B. S. Li, R. Akimoto, K. Akita, T. Hasama, "Structural study of (CdS/ZnSe)/BeTe superlattices for λ = 1.55 μm intersubband transition," *J. Appl. Phys.* **95**, 5352-5359 (2004).

[98] S. R. Forrest, "Optical detectors: Three contenders," *Spectrum* **23**, 76-84 (1986).

[99] G. E. Stillman and C. M. Wolfe, "Avalanche photodiodes," In Semiconductors and Semimetals vol. 12: *Infrared Detectors II*, ed. R.K. Willardson and A.C. Beer, Chapter 5, Academic Press, New York, 1977.

[100] S. M. Sze, *Physics of semiconductor devices*, 2nd ed. Wiley, New York, 1981.

[101] F. Omnes, N. Marenco, B. Beaumont, Ph. de Mierry, E. Monroy, F. Calle, and E. Munoz, "Metalorganic vapor-phase epitaxy-grown AlGaN materials for visible-blind ultraviolet photodetector applications," *J. Appl. Phys.* **86**, 5286-5292 (1999).

[102] R. McClintock, A. Yasan, K. Mayes, D. Shiell, S. R. Darvish, P. Kung, and M. Razegh, "High quantum efficiency AlGaN solar-blind *p-i-n* photodiodes," *Appl. Phys. Lett.* **84**, 1248-1250 (2004).

[103] H. Kressel and J. K. Butler, *Semiconductor Lasers and Heterojunction LEDs*, Academic Press, New York, 1977.

[104] R. G.. Seippel, *Optoelectronics for technology and engineering*, Prentice-Hall, Englewood Cliffs, NJ, 1989.

[105] C. H. Chen, S. J. Chang, Y. K. Su, J. K. Sheu, J. F. Chen, C. H. Kuo and Y. C. Lin, "Nitride-based cascade near white light-emitting diodes," *IEEE Photon. Technol. Lett.* **14**, 908-910 (2002).

[106] S. Kamiyama, M. Iwaya, S. Takanami, S. Terao, A. Miyazaki, H. Amano, and I. Akasaki, "UV Light-Emitting Diode Fabricated on Hetero-ELO-Grown $Al_{0.22}Ga_{0.78}N$ with Low Dislocation Density", *phys. stat. sol.* (a) **192**, 296-300, (2002).

[107] G. P. Agrawal and N. K. Dutta, *Long wavelength semiconductor lasers*, Van Nostrand Reinhold, New York, 1986.

[108] J. Singh, *Physics of semiconductors and their heterostructures*, McGraw-Hill, New York, 1993.

[109] I. Akasaki, S. Sota, H. Sakai, T. Tanaka, M. Koike, and H. Amano, "Shortest wavelength semiconductor laser diode," *Electron. Lett.* **32**, 1105-1106 (1996).

[110] S. Nakamura, et al., "InGaN-Based Multi-Quantum-Well-Structure Laser Diodes," *Jpn. J. Appl. Phys.* **35**, L74-L76 (1996).

[111] S. Nakamura, et al. "Room-temperature continuous-wave operation of InGaN multi-quantum-well structure laser diodes," *Appl. Phys. Lett.* **69**, 4056-4058 (1996).

[112] B. K. Ridley, "Electron scattering by confined LO polar phonons in a quantum well," *Phys. Rev. B* **39**, 5282-5286 (1989).

[113] T. Asano, S. Noda, and K. Tomoda, "Pump & probe measurement of intersubband relaxtion time in short wavelength intersubband transition," *Appl. Phys. Lett.* **74**, 1418-1420 (1999).

[114] T. Asano, M. Tamura, S. Yoshizawa, and S. Noda, "Pump-probe measurement of ultrafast all-optical modulation based on intersubband transition in *n*-doped quantum wells," *Appl. Phys. Lett.* **77**, 19-21 (2000).

[115] T. Asano, S. Yoshizawa, and S. Noda, "Carrier relaxation dynamics in an ultrafast all-optical modulator using an intersubband transition," *Appl. Phys. Lett.* **79**, 4509-4511 (2000).

[116] G. Reuscher, M. Keim, H.J. Lugauer, A. Waag, G. Landwehr, "ZnSe/BeTe Type-II Light Emitting Diodes," *phys. stat. sol.* (a) **180**, 225-229 (2000).

[117] S. Strite and H. Morkoc, "GaN, AlN, and InN: A review," *J. Vac. Sci. Technol.* B **10**, 1237-1266 (1992).

[118] C. R. Abernathy, *GaN and Related Materials*, edited by S. J. Pearton, Gordon and Breach, New York, 1997.

[119] S. Yoshida, S. Misawa, S. Gonda, "Epitaxial growth of GaN/AlN heterostructures," *J. Vac. Sci. Technol.* B **1**, 250-253 (1983).

[120] M. Hashimoto, H. Amano, N. Sawaki, and I. Akasaki, "Effects of hydrogen in an ambient on the crystal growth of GaN using $Ga(CH_3)_3$ and NH_3," *J. Crystal Growth* **68**, 163-168 (1984).

[121] H. Amano, N. Sawaki, I. Akasaki and Y. Toyoda, "Metalorganic vapor phase

epitaxial growth of a high quality GaN film using an AlN buffer layer," *Appl. Phys. Lett.* **48**, 353-355 (1986).

[122] I. Akasaki, H. Amano, Y. Koide, K. Hiramatsu, and N. Sawaki, "Effects of ain buffer layer on crystallographic structure and on electrical and optical properties of GaN and $Ga_{1-x}Al_xN$ ($0 < x \leqq 0.4$) films grown on sapphire substrate by MOVPE ," *J. Crystal Growth* **98**, 209-219 (1989).

[123] H. Amano, I. Akasaki, K. Hiramatsu, and N. Koide, "Effects of the buffer layer in metalorganic vapour phase epitaxy of GaN on sapphire substrate," *Thin Solid Films* **163**, 415-420 (1988).

[124] H. Amano, T. Asaki, and I. Akasaki, "Stimulated Emission Near Ultraviolet at Room Temperature from a GaN Film Grown on Sapphire by MOVPE Using an AlN Buffer Layer," *Jpn. J. Appl. Phys.* **29**, L205-L206 (1990).

[125] S. Nakamura, "GaN Growth Using GaN Buffer Layer," *Jpn. J. Appl. Phys.* **30**, L1705-L1707 (1991).

[126] S. Nakamura, M. Senoh, and T. Mukai, "Highly P-Typed Mg-Doped GaN Films Grown with GaN Buffer Layers," *Jpn. J. Appl. Phys.* **30**, L1708-L1711 (1991).

[127] S. Nakamura, "Analysis of Real-Time Monitoring Using Interference Effects," Jpn, *J. Appl. Phys.* **30**, 1348-1353 (1991).

[128] S. Nakamura, "*In Situ* Monitoring of GaN Growth Using Interference Effects," Jpn, *J. Appl. Phys.* **30**, 1620-1627 (1991).

[129] M. Mesrine, N. Grandjean, and J. Massies, "Efficiency of NH_3 as nitrogen source for GaN molecular beam epitaxy," *Appl. Phys. Lett.* **72**, 350-352 (1998).

[130] X. Q. Shen, et al, "Realization of Ga-polarity GaN films in radio-frequency plasma-assisted molecular beam epitaxy," *J. Crystal Growth* **218**, 155-160 (2000).

[131] S. Nakamura, S. Pearton, and G. Fasol, *The Blue Laser Diode*, Springer, New York, 2000.

[132] T. Sasaki, T. Matsuoka, "Analysis of two-step-growth conditions for GaN on an AlN buffer layer," *J. Appl. Phys.* **77**, 192-200 (1995).

[133] S. Nakamura, and S. F. Chichibu, *Introduction to Nitride semiconductor blue lasers and light emitting diodes*, Taylor & Francis, London 2000.

[134] K. Kaneko, N. Iizuka, and N. Suzuki, "Effect of Intermediated Layers in

$Al_{0.65}Ga_{0.35}N$/GaN Multiple Quantum Wells," *Proc. Int. Workshop on Nitride Semiconductors (IWN 2000)*, PMD-30, 129-132 (2000).

[135] A. Kikuchi, et al, "Improvement of crystalline quality of RF-plasma-assisted molecular beam epitaxy grown Ga-polarity GaN by high-temperature grown AlN multiple intermediate layers," *Jpn. J. Appl. Phys.* **39**, L330-L333 (2000).

[136] E. Feltin, B. Beaumont, M. Laugt, P. De Mierry, P. Vennegues, H. Lahreche, M. Leroux, and P. Gibart, "Stress control in GaN grown on silicon (111) by metalorganic vapor phase epitaxy," *Appl. Phys. Lett.* **79**, 3230-3232 (2001).

[137] H. Hirayama, M. Ainoya, A. Kinoshita, A. Hirata, and T. Aoyagi, "Fabrication of a low-threading-dislocation-density $Al_xGa_{1-x}N$ buffer on SiC using highly Si-doped $Al_xGa_{1-x}N$ superlattices," *Appl. Phys. Lett.* **80**, 2057-2059 (2002).

[138] H.-M. Wang, J.-P. Zhang, C.-Q. Chen, Q. Fareed, J.-W. Yang, "AlN/AlGaN superlattices as dislocation filter for low-threading-dislocation thick AlGaN layers on sapphire," *Appl. Phys. Lett.* **81**, 604-606 (2002).

[139] T. Someya, K. Hoshino, J. C. Harris, K. Tachibana, and Y. Arakawa, "Photoluminescence from sub-monolayer-thick GaN/AlGaN quantum wells", *Appl. Phys. Lett.* **77**, 1336-1338 (2000).

[140] S. Yamaguchi, M. Kosaki, Y. Watanabe, Y. Yukawa, S. Nitta, H. Amano, and I. Akasaki, "Metalorganic vapor phase epitaxy growth of crack-free AlN on GaN and its application to high-mobility AlN/GaN superlattices," *Appl. Phys. Lett.* **79**, 3062-3064 (2001).

[141] S. Yamaguchi, Y. Iwamura, M. Kosaki, Y. Watanabe, Y. Yukawa, S. Nitta, S. Kamiyama, H. Amano and I. Akasaki, "Electrical properties of strained AlN/GaN superlattices on GaN grown by metalorganic vapor phase epitaxy," *Appl. Phys. Lett.* **80**, 802-804 (2002).

[142] I. Waki, C. Kumtornkittikul, K. Sato, Y. Shimogaki, and Y. Nakano, "Characterization of crack-free AlN/GaN multiple quantum wells grown by metalorganic vapor phase epitaxy using H_2 as a carrier gas," *phys. stat. sol.* (b) **234**, 961-964 (2002).

[143] K. Hoshino, T. Someya, K. Hirakawa, and Y. Arakawa, "Low-pressure MOCVD growth of GaN/AlGaN multiple quantum wells for intersubband transitions," J. Crystal Growth **237**, 1163-1166 (2002).

[144] N. Zhou, S. A. Lowry, A. Krishnan, "CFD simulation of pulsed MOCVD to reduce gas-phase parasitic reaction," Proc. SPIE **3792**, 58-72, Materials Research in Low Gravity II (1999).

[145] J. R. Creighton, G. T. Wang, W. G. Breiland, M. E. Coltrin, I.-T. Im, H.-J. Oh, M. Sugiyama, Y. Nakano, and Y. Shimogaki, "Nature of the parasitic chemistry during AlGaInN OMVPE: Fundamental kinetics determining growth rate profiles of InP and GaAs in MOCVD with horizontal reactor," *J. Crystal Growth* **261**, 204-213 (2004).

[146] H. C. Liu, M. Buchanan, and Z. R. Wasilewski, "How good is the polarization selection rule for intersubband transitions?," *Appl. Phys. Lett.* **72**, 1682-1684 (1998).

[147] M. J. Kane, M. T. Emeny, N. Apsley, C. R. Whitehouse, and D. Lee, "Inter-sub-band absorption in GaAs/AlGaAs single quantum wells," *Semicond. Sci. Technol.* **3**, 722-725 (1988).

[148] M. Horowitz, Y. Barad, and Y. Silberberg, "Noiselike pulses with a broadband spectrum generated from an erbium-doped fiber laser," *Opt. Lett.* **22**, 799-801 (1997).

[149] Y. Takushima, F. Futami, and K. Kikuchi, "Generation of over 140-nm-wide super-continuum from a normal dispersion fiber by using a mode-locked semiconductor laser source," *IEEE Photon. Technol. Lett.* **10**, 1560-1562 (1998).

[150] N. Nishizawa and T. Goto, "Widely broadened supercontinuum generation using a highly nonlinear dispersion shifted fibers and femtosecond fiber laser," *Jpn. J. Appl. Phys.* **40**, L365-L367 (2001).

[151] F.O. Ilday, F.W. Wise, and T. Sosnowski, "High-energy femtosecond stretched-pulse fiber laser with nonlinear optical loop mirror," *Opt. Lett.* **27**, 1531-1533 (2002).

[152] Y. Ozeki, K. Taira, K. Aiso, Y. Takushima and K. Kikuchi, "Highly flat super-continuum generation from 2 ps pulses using 1 km-long erbium-doped fibre amplifier," *Electron. Lett.* **38**, 1642-1643 (2002).

[153] C. Gmachl, D. L. Sivco, R. Colombelli, F. Capasso, and A. Y. Cho, "Ultra-Broadband Semiconductor Laser," *Nature* **415**, 883 (2002).

[154] J.W. Nicholson, et al, "All-fiber octave-spanning supercontinuum," *Opt. Lett.* **28**,

643-645 (2003).

[155] Y. Takushima, K. Yasunaka, Y. Ozeki and K. Kikuchi, "87 nm bandwidth noise-like pulse generation from erbium-doped fibre laser," *Electron. Lett.* **41**, 399-340 (2005).

[156] J.M. Li, et al, "Effect of spontaneous and piezoelectric polarization on intersubband transition in AlxGa1-xN/GaN quantum well," *J. Vac. Sci. Technol.* B **22**, 2568-2573 (2004).

[157] N. Suzuki, N. Iizuka and K. Kaneko, "Calculation of near-infrared intersubband absorption spectra in GaN/AlN quantum wells," *Jpn. J. Appl. Phys.* **42**, 132-139 (2003).

[158] K. A. Mkhoyan, J. Silcox, H. Wu, W. J. Schaff, and L. F. Eastman, "Nonuniformities in GaN/AlN quantum wells," *Appl. Phys. Lett.* **83**, 2668-2670 (2003).

[159] S. Tsujino, et al., "Interface-roughness-induced broadening of intersubband electroluminescence in *p*-SiGe and *n*-GaInAs/AlInAs quantum-cascade structures," *Appl. Phys. Lett.* **86**, 062113 (2005).

[160] M. Asif Khan, R. A. Skogman, J. M. Van Hove, D. T. Olson, and J. N. Kuzina, "Atomic layer epitaxy of GaN over sapphire using switched metalorganic chemical vapor deposition," *Appl. Phys. Lett.* **60**, 1366 (1992).

[161] M. Asif Khan, J. N. Kuzina, R. A. Skogman, D. T. Olson, M. MacMillan, and W. J. Choyke, "Low pressure metalorganic chemical vapor deposition of AIN over sapphire substrates," *Appl. Phys. Lett.* **61**, 2539 (1992).

[162] M. Asif Khan, J. N. Kuzina, D. T. Olson, T. George, and W. T. Pike, "GaN/AlN digital alloy short-period superlattices by switched atomic layer metalorganic chemical vapor deposition," *Appl. Phys. Lett.* **63**, 3470 (1993).

[163] J. Zhang, E. Kuokstis, Q. Fareed, H. Wang, J. Yang, G. Simin, and M. Asif Khan, R. Gaska and M. Shur, "Pulsed atomic layer epitaxy of quaternary AlInGaN layers," *Appl. Phys. Lett.* **79**, 925-927 (2001).

[164] J. P. Zhang, M. Asif Khan, W. H. Sun, H. M. Wang, C. Q. Chen, Q. Fareed, E. Kuokstis, and J. W. Yang, "Pulsed atomic-layer epitaxy of ultrahigh-quality $Al_xGa_{1-x}N$ structures for deep ultraviolet emissions below 230 nm," *Appl. Phys. Lett.* **81**, 4392-4394 (2002).

[165] C. Adelmann, J. Brault, J.-L. Rouvière, H. Mariette, G. Mula, and B. Daudin, "Atomic-layer epitaxy of GaN quantum wells and quantum dots on (0001) AlN," *J. Appl. Phys.* **91**, 5498-5500 (2002).

[166] M. Hiroki and N. Kobayashi, "Flat surfaces and interfaces in AlN/GaN heterostructures and superlattices grown by flow-rate modulation epitaxy," *Jpn. J. Appl. Phys.* **42**, 2305-2308 (2003).

[167] Y.-J. Lee and S.-W. Kang, "Growth of aluminum nitride thin films prepared by plasma-enhanced atomic layer deposition," *Thin Solid Films* **446**, 227-231 (2004).

[168] R. Hui, S. Taherion, Y. Wan, J. Li, S. X. Jin, J. Y. Lin, and H. X. Jiang, "GaN-based waveguide devices for long-wavelength optical communications," *Appl. Phys. Lett.* **82**, 1326-1328 (2003).

[169] N. Li, I. Waki, C. Kumtornkittikul, J. Liang, M. Sugiyama, Y. Shimogaki, and Y. Nakano, "Fabrication of AlGaN-based waveguides by inductively coupled plasma etching," *Jpn. J. Appl. Phys.* **43**, L1340-L1342 (2004).

[170] L. B. Chang, S. S. Liu, and M. J. Jeng, "Etching Selectivity and Surface Profile of GaN in the Ni, SiO_2 and Photoresist Masks Using an Inductively Coupled Plasma," *Jpn. J. Appl. Phys.* **40**, 1242-1243 (2001).

[171] K. Tamura, L. E. Nelson, H.A. Haus, and E. P. Ippen, "Soliton versus nonsoliton operation of fiber ring lasers," *Appl. Phys. Lett.* **64**, 149-151 (1994).

[172] N. Iizuka, K. Kaneko, and N. Suzuki, "Time-Resolved Characterization of All-Optical Switch Utilizing GaN Intersubband Transition," *International Quantum Electronics Conference 2005 and the Pacific Rim Conference on Lasers and Electro-Optics (IQEC/CLEO-PR) 2005*, CThM2-3 (2005).

[173] Y. Ohba, and R. Sato, "Growth of AlN on sapphire substrates by using a thin AlN buffer layer grown two-dimensionally at a very low V/III ratio," *J. Crystal Growth* **221**, 258-261 (2000).

[174] Y. Ohba and A. Hatano, "Growth of High-Quality AlN and AlN/GaN/AlN Heterostructure on Sapphire Substrate," *Jpn. J. Appl. Phys.* **35**, L1013-L1015 (1996).

[175] M. Miyamura, K. Tachibana, T. Someya, and Y. Arakawa, "Self-assembled growth of GaN quantum dots using low-pressure MOCVD," *phys. stat. sol.* (b)

228, 191-194 (2001).

[176] S. Gupta, J. F. Whitaker, and G. A. Mourou, "Ultrafast carrier dynamics in III-V semiconductors grown by molecular-beam epitaxy at very low substrate temperatures," *IEEE J. Quantum Electron.* **28**, 2464-2472 (1992).

[177] R. Takahashi, H. Itoh, and H. Iwamura, "Ultrafast 1.55 μm all-optical switching using low-temperature-grown multiple quantum wells," Ultrafast high-contrast all-optical switching using spin polarization in low-temperature-grown multiple quantum wells," *Appl. Phys. Lett.* **68**, 153-155 (1996).

[178] R. Takahashi, H. Itoh, and H. Iwamura, "Ultrafast high-contrast all-optical switching using spin polarization in low-temperature-grown multiple quantum wells," *Appl. Phys. Lett.* **77**, 2958-2960 (2000).

[179] R. Takahashi, "Low-temperature-grown surface-reflection all-optical switch (LOTOS)," *Opt. Quantum Electron.* **33**, 999-1017 (2001).

[180] R. Takahashi, T. Nakahara, H. Takenouchi, T. Yasui, and H. Suzuki, "Ultrafast all-optical serial-to-parallel conversion and its application to optical label processing," *Opt. Rev.* **11**, 98-105 (2004).

[181] S. Kodama, T. Ito, N. Watanabe, S. Kondo, H. Takeuchi, H. Ito, T. Ishibashi, "200 Gbit/s monolithic photodiode-electroabsorption modulator (PD-EAM) optical gate," *59th Annual Device Research Conference (DRC 2001)*, 151-152 (2001).

[182] O. Wada, "Femtosecond semiconductor-based optoelectronic devices for optical communications systems," *Opt. Quantum Electron.* **32**, 453-471 (2000).

[183] L. I. Schiff, *Quantum Mechanics*, 2nd ed., McGraw-Hill, New York, 1968.

[184] S. L. Chuang, *Physics of Optoelectronic Devices*, Wiley, New York, 1995.

[185] H. Haken, *Light*, Vol.1, *Waves, Photons, Atoms*, North-Holland, Amsterdam, 1986.

[186] D. Ahn and S. L. Chuang, "Calculation of linear and nonlinear intersubband optical absorptions in a quantum well model with an applied electric field," *IEEE J. Quantum Electron.* **QE-23**, 2196-2204 (1987).

[187] O. Ambacher, B. Foutz, J. Smart, J. R. Shealy, N. G. Weimann, K. Chu, M. Murphy, A. J. Sierakowski, W. J. Schaff, L. F. Eastman, R. Dimitrov, A. Mitchell, and M. Stutzmann, "Two dimensional electron gases induced by spontaneous

and piezoelectric polarization in undoped and doped AlGaN/GaN heterostructures," *J. Appl. Phys.* **87**, 334 (2000).

[188] F. Bernardini, V. Fiorentini, and D. Vanderbilt, "Spontaneous polarization and piezoelectric constants of III-V nitrides," *Phys. Rev. B* **56**, R10024-R10027 (1997).

PUBLICATION LIST

Technical Journals

1. Chaiyasit Kumtornkittikul, Masakazu Sugiyama, and Yoshiaki Nakano, "GaN/AlN multiple quantum wells grown on GaN-AlN waveguide structures by metalorganic vapor phase epitaxy," *J. Electron. Mater.* (2006). (*in press*)
2. Ning Li, Ichitaro Waki, Chaiyasit Kumtornkittikul, Ji-Hao Liang, Masakazu Sugiyama, Yukihiro Shimogaki, and Yoshiaki Nakano, "Fabrication of AlGaN-based waveguides by inductively coupled plasma etching," *Jpn. J. Appl. Phys.* **43**, L1340-L1342 (2004).
3. Ichitaro Waki, Chaiyasit Kumtornkittikul, Yukihiro Shimogaki, and Yoshiaki Nakano, "Shortest intersubband transition wavelength (1.68 μm) achieved in AlN/GaN multiple quantum wells by metalorganic vapor phase epitaxy," *Appl. Phys. Lett.* **82**, 4465-4467 (2003), and Errata, *Appl. Phys. Lett.* **84**, 3703 (2004).
4. Ichitaro Waki, Chaiyasit Kumtornkittikul, Kentaro Sato, Yukihiro Shimogaki, and Yoshiaki Nakano, "Characterization of crack-free AlN/GaN multiple quantum wells grown by metalorganic vapor phase epitaxy using H_2 as a carrier gas," *phys. stat. sol.* (b) **234**, 961-964 (2002).
5. Chaiyasit Kumtornkittikul, Masakazu Sugiyama, Yukihiro Shimogaki, and Yoshiaki Nakano, "Intersubband Absorption in GaN/AlN multiple quantum wells grown by metalorganic vapor phase epitaxy," in preparation to submit to *Jpn. J. Appl. Phys.*
6. Chaiyasit Kumtornkittikul and Yoshiaki Nakano, "Intersubband absorption measurements in waveguide using supercontinuum light source," in preparation to submit to *Electron. Lett.*
7. Chaiyasit Kumtornkittikul, Norio Iizuka, Nobuo Suzuki, and Yoshiaki Nakano, "Ultrafast all-optical switch utilizing intersubband transition in GaN/AlN quantum wells with AlN waveguide," in preparation to submit to *IEEE Photon. Technol. Lett.*

International Conferences

8. Chaiyasit Kumtornkittikul, Norio Iizuka, Nobuo Suzuki, and Yoshiaki Nakano, "Intersubband transition devices using AlN waveguide and GaN/AlN quantum wells," to be presented in *Conference on Lasers and Electro-Optics / Quantum Electronics and Laser Science Conference (CLEO/QELS 2006)*, May 2006.
9. Chaiyasit Kumtornkittikul, Masakazu Sugiyama, and Yoshiaki Nakano, "GaN waveguide structures with AlN cladding for novel optical devices," *6th International Conference on Nitride Semiconductors (ICNS-6)*, MO-P-013, Bremen, Germany, Aug 28-Sep 2, 2005.
10. Chaiyasit Kumtornkittikul, Masakazu Sugiyama, and Yoshiaki Nakano, "AlN high-mesa waveguides for ultrafast intersubband transition devices," *10th OptoElectronics and Communications Conference (OECC 2005)*, 8E1-5, pp. 844-845, Seoul, Korea, Jul 4-8, 2005.
11. Chaiyasit Kumtornkittikul, Masakazu Sugiyama, and Yoshiaki Nakano, "GaN/AlN multiple quantum wells grown on GaN-AlN waveguide structures by metalorganic vapor phase epitaxy," *47th Electronic Materials Conference (EMC 2005)*, BB5, Santa Barbara, CA, Jun 22-24, 2005.
12. Chaiyasit Kumtornkittikul, Ichitaro Waki, Ning Li, Hiroshi Otani, Masakazu Sugiyama, Yukihiro Shimogaki, and Yoshiaki Nakano, "Waveguide structure for ultrafast photonic devices utilizing intersubband absorption in GaN-based MOVPE-grown multiple quantum wells," *IEEE Lasers and Electro-Optics Society Annual Meeting (LEOS 2004)*, MO4, pp. 140-141, Puerto Rico, USA, Nov 7-11, 2004.
13. Chaiyasit Kumtornkittikul, Ichitaro Waki, Ning Li, Masakazu Sugiyama, Yukihiro Shimogaki, and Yoshiaki Nakano, "GaN/AlN multiple quantum wells and waveguide fabrication for ultrafast photonic devices utilizing intersubband transition," *IEEE TENCON 2004*, TD-10-2, 0899, pp. 140-143, Chiangmai, Thailand, Nov 21-24, 2004.
14. Ichitaro Waki, Chaiyasit Kumtornkittikul, Yukihiro Shimogaki, and Yoshiaki Nakano, "Non-uniform distribution of intersubband transition wavelength in

MOVPE-grown AlN/GaN multiple quantum wells over a 2-inch sapphire substrate," *2003 Material Research Society Fall Meeting (MRS)*, Y10.54, Boston, MA, Dec 1-5, 2003.

15. Chaiyasit Kumtornkittikul, Ichitaro Waki, Yukihiro Shimogaki, and Yoshiaki Nakano, "First observation of 1.55 μm intersubband absorption in MOVPE-grown AlN/GaN multiple quantum wells," *IEEE Lasers and Electro-Optics Society Annual Meeting (LEOS 2003)*, ThU3, pp. 947-948, Tucson, Arizona, Oct 26-30, 2003.
16. Ichitaro Waki, Chaiyasit Kumtornkittikul, Yukihiro Shimogaki, and Yoshiaki Nakano, "Effect of AlN/GaN superlattices in reducing dislocation density in GaN grown by MOVPE," Meeting Abstracts, *204th Electrochemical Society Annual Meeting (ECS)*, Abs. 949, Orlando, Florida, Oct 12-17, 2003.
17. Chaiyasit Kumtornkittikul, Ichitaro Waki, Yukihiro Shimogaki, and Yoshiaki Nakano, "Experimental and theoretical study of intersubband absorption in MOVPE-grown Al(Ga)N/GaN multiple quantum wells," *10th International Workshop on Femtosecond Technology (FST 2003)*, Makuhari, Japan, Jul 16-17, 2003.
18. Ichitaro Waki, Chaiyasit Kumtornkittikul, Yukihiro Shimogaki, and Yoshiaki Nakano, "Near-infrared intersubband transitions in MOVPE-grown AlN/GaN multiple quantum wells," *10th International Workshop on Femtosecond Technology (FST 2003)*, WB-2, Makuhari, Japan, Jul 16-17, 2003.
19. Chaiyasit Kumtornkittikul, Ichitaro Waki, Yukihiro Shimogaki, and Yoshiaki Nakano, "Well and barrier width dependence of near-infrared intersubband absorption in AlN/GaN multiple quantum wells grown by MOVPE," *5th International Conference on Nitride Semiconductors (ICNS-5)*, Mo-P1.047, p. 244, Nara, Japan, May 25-30, 2003.
20. Ichitaro Waki, Chaiyasit Kumtornkittikul, Yukihiro Shimogaki, and Yoshiaki Nakano, "Achievement of shortest intersubband transition wavelength (1.68 μm) in MOVPE-grown Al(Ga)N/GaN MQW systems," *5th International Conference on Nitride Semiconductors (ICNS-5)*, Tu-B2.5, p. 84, Nara, Japan, May 25-30, 2003.
21. Ichitaro Waki, Chaiyasit Kumtornkittikul, Kentaro Sato, Yukihiro Shimogaki, and Yoshiaki Nakano , "Characterization of crack-free AlN/GaN multiple quantum wells grown by metalorganic vapor phase epitaxy using H_2 as a carrier gas", *International*

Workshop on Nitride Semiconductors (IWN 2002), Paper 368, p. 372, Archen, Germany, Jul 22-25, 2002.

Domestic Conferences

22. Chaiyasit Kumtornkittikul, 飯塚紀夫, 鈴木信夫, 中野義昭, "AlN 導波路型 GaN/AlN 量子井戸サブバンド間遷移を用いた超高速全光スイッチの作製 (Fabrication of ultrafast all-optical switch utilizing intersubband transition in GaN/AlN quantum wells with AlN waveguide)," 第 53 回応用物理学関係連合講演会(武蔵工業大学), 2006 年 3 月. (発表予定)
23. Jung-Seung Yang, Chaiyasit Kumtornkittikul, Takaaki Orii, Masakazu Sugiyama, Yoshiaki Nakano, and Yukihiro Shimogaki, "MOVPE Growth of AlN by Pulse Injection Method and Improvement of Crystalline Quality," 2005 Korea-Japan Joint Workshop on Advanced Semiconductor Process and Equipments, Korea.
24. Chaiyasit Kumtornkittikul, 杉山正和, 中野義昭, "サブバンド間遷移超高速光スイッチに向けた AlN ハイメサ導波路の作製(Fabrication of AlN high-mesa waveguide for ultrafast optical switch using intersubband transition)," 第 66 回応用物理学会学術講演会(徳島大学), 8a-T-28, 2005 年 9 月.
25. 梁正承, Chaiyasit Kumtornkittikul, 杉山正和, 中野義昭, 霜垣幸浩, "Pulse Injection Method による AlN の成長と結晶性の向上(MOVPE growth of AlN by pulse injection method and improvement of crystallinity)," 第 66 回応用物理学会学術講演会(徳島大学), 8a-X-12, 2005 年 9 月.
26. 大谷洋, Chaiyasit Kumtornkittikul, 杉山正和, 中野義昭, "MOVPE 成長 GaN/AlN 多重量子井戸中のサブバンド間遷移に寄与する電子密度の評価 (Estimation of carrier density contributing to intersuband transition in AlN/GaN MQWs grown by MOVPE)," 第 52 回応用物理学関係連合講演会(埼玉大学), 31p-L-2, 2005 年 3 月.
27. Chaiyasit Kumtornkittikul, リ・ニン, 脇一太郎, 大谷洋, 杉山正和, 中野義昭, "GaN 系サブバンド間吸収超高速光デバイスに向けた導波路の設計 (GaN-based waveguide structure for ultrafast photonic devices utilizing

intersubband absorption),” 電子情報通信学会エレクトロニクスソサイエティ大会(徳島大学), C-4-17, p. 271, 2004 年 9 月.

28. 李寧, Chaiyasit Kumtornkittikul, 脇一太郎, 杉山正和, 霜垣幸浩, 中野義昭, “塩素系 ICP エッチングによる GaN 導波路の作製(Fabrication of GaN waveguides using Cl_2-based inductively coupled plasma etching),” 第 51 回応用物理学関係連合講演会(東京工科大学), 30a-ZV-7, 2004 年 3 月 30 日.
29. Chaiyasit Kumtornkittikul, 脇一太郎, 霜垣幸浩, 中野義昭, “MOVPE 成長 AlN/GaN 多重量子井戸における 1.55 μm のサブバンド間遷移(Intersubband transition at λ~1.55 μm in MOVPE-grown AlN/GaN multiple quantum wells), 電子情報通信学会エレクトロニクスソサイエティ大会(新潟大学), C-4-17, p. 293, 2003 年 9 月 25 日.
30. Chaiyasit Kumtornkittikul, 脇一太郎, 霜垣幸浩, 中野義昭, “MOVPE 成長 AlN/GaN 多重量子井戸における 1.55μm サブバンド間吸収の観測(Achievement of intersubband absorption at λ~1.55 μm in MOVPE-grown AlN/GaN multiple quantum wells),” 第 64 回応用物理学会学術講演会(福岡大学), 30p-YH-7, 2003 年 8 月.
31. 脇一太郎, Chaiyasit Kumtornkittikul, 霜垣幸浩, 中野義昭, “MOVPE 成長 AlN/GaN 多重量子井戸における近赤外サブバンド間遷移(Near-infrared intersubband transitions in MOVPE-grown AlN/GaN MQWs),” 第 64 回応用物理学会学術講演会(福岡大学), 1a-G-5, 2003 年 9 月.
32. Chaiyasit Kumtornkittikul, Ichitaro Waki, Yukihiro Shimogaki, and Yoshiaki Nakano, “Experimental and theoretical study of intersubband absorption in MOVPE-grown Al(Ga)N/GaN multiple quantum wells,” *22nd Electronic Materials Symposium (EMS-22)*, H9, pp. 267-268, Biwako, Shiga, Jul 2-4, 2003.
33. Ichitaro Waki, Chaiyasit Kumtornkittikul, Yukihiro Shimogaki, and Yoshiaki Nakano, “Near-infrared intersubband absorption in Al(Ga)N/GaN multiple quantum wells grown by MOVPE,” *22nd Electronic Materials Symposium (EMS-22)*, H8, pp. 265-266, Biwako, Shiga, Jul 2-4, 2003.
34. Chaiyasit Kumtornkittikul, 脇一太郎, 霜垣幸浩, 中野義昭, “MOVPE 成長 AlN/GaN 多重量子井戸におけるサブバンド間吸収の量子井戸及び障壁幅依存性(Well and barrier width dependence of intersubband absorption in AlN/GaN MQWs grown by MOVPE),” 第 50 回応用物理学関係連合講演会(神奈川大学),

29a-ZK-5, 2003 年 3 月.

35. 脇一太郎, Chaiyasit Kumtornkittikul, 霜垣幸浩, 中野義昭, "MOVPE 成長 Al(Ga)N/GaN 多重量子井戸における最短波長(1.68 μm)サブバンド間遷移の観測 (Achievement of shortest intersubband transition wavelength (1.68μm) in MOVPE-grown Al(Ga)N/GaN MQW systems)," 第 50 回応用物理学関係連合講演会(神奈川大学), 29p-V-9, 2003 年 3 月.
36. Chaiyasit Kumtornkittikul, 脇一太郎, 霜垣幸浩, 中野義昭, "サブバンド間遷移応用に向けた AlN/GaN 多重量子井戸構造の MOVPE 成長 (MOVPE growth of AlN/GaN MQW structures for intersubband transition applications)," 第 63 回応用物理学会学術講演会(新潟大学), 25a-YH-9, 2002 年 9 月.
37. 脇一太郎, Chaiyasit Kumtornkittikul, 霜垣幸浩, 中野義昭, "AlN/GaN 超格子による転位密度の低減(Reduction of dislocation density using AlN/GaN super-lattices),"第 63 回応用物理学会学術講演会(新潟大学), 24p-YH-7, 2002 年 9 月.
38. Ichitaro Waki, Chaiyasit Kumtornkittikul, Kentaro Sato, Yukihiro Shimogaki, and Yoshiaki Nakano, "Metal-organic vapor phase epitaxial growth of crack-free AlN/GaN multiple quantum wells and their characterization," *21st Electronic Materials Symposium (EMS-21)*, C5, pp. 53-54, Izu-Nagaoka, Jun 19-21, 2002.

Publications Related to Electroabsorption Modulator

39. Zhou Xiaoping, Hiromasa Shimizu, Chaiyasit Kumtornkittikul,and Yoshiaki Nakano, "Wavelength Conversion using Polarization Dependence of Cross-phase Modulation in an InGaAlAs Multiple-quantum-well Electroabsorption Modulator," *17th InP & Related Materials Conference (IPRM'2005)*, MOB-1-5, Glasgow, UK, May 8-12, 2005.
40. Masaki Kato, Chaiyasit Kumtornkittikul, and Yoshiaki Nakano, "Wavelength Conversion Using Polarization Dependence of Photo-Induced Phase Shift in an InGaAsP MQW-EA Modulator," *Optical Fiber Communication Conference (OFC 2002)*, ThDD3, pp. 595-596, Anaheim, CA, Mar 17-22, 2002.

41. 加藤正樹、金子慎、Chaiyasit Kumtornkittikul, 中野義昭、“MQW-EA 変調器における光誘起屈折変化の偏光依存性を用いた波長変換(II) (Wavelength conversion using polarization-dependence of photo-induced refractive index change in an MQW-EA modulator II),” 第 49 回応用物理関連連合講演会(東海大学), 29p-ZS-18, 2002 年 3 月.